SAND2019-13643C

Thermal Processing Effects on Heat Affected Zone Liquation Cracking Susceptibility of Boron Micro-alloyed 304L Stainless Steel

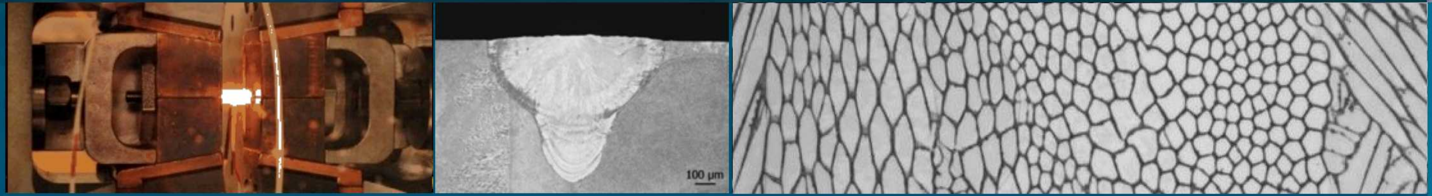

PRESENTED BY

Jeff Rodelas, Don Susan, Mike Maguire, Peter Duran, Matt, Vieira, Alex Barr, Alex Hickman, Cele Jaramillo, Christina Profazi

Metallurgy & Material Joining Department

Sandia National Laboratories, Albuquerque, NM

November 12th, 2019

American Welding Society 2019 Professional Program: Welding Metallurgy I

Sandia National Laboratories is a multimission laboratory managed and operated by National Technology & Engineering Solutions of Sandia, LLC, a wholly owned subsidiary of Honeywell International Inc., for the U.S. Department of Energy's National Nuclear Security Administration under contract DE-NA0003525.

SAND2019-XXXXC

Stringent control of 304L alloy composition is the cornerstone for mitigation of hot cracking risk

- Majority of prior work on 304L hot cracking is focused on solidification cracking
- Comparatively fewer established compositional relationships for HAZ liquation cracking.
- Weld-Critical (WC) austenitic stainless steels have common features designed to optimize weldability
  - Secondary remelting. This can be via VAR, VIM/VAR, or ESR
  - Tight control of impurities including S, P, O, N, **B**
  - Cr_{eq}/Ni_{eq} limits to control weld solidification behavior

Modified Suutala Weldability Diagram for Various WC 304L specifications

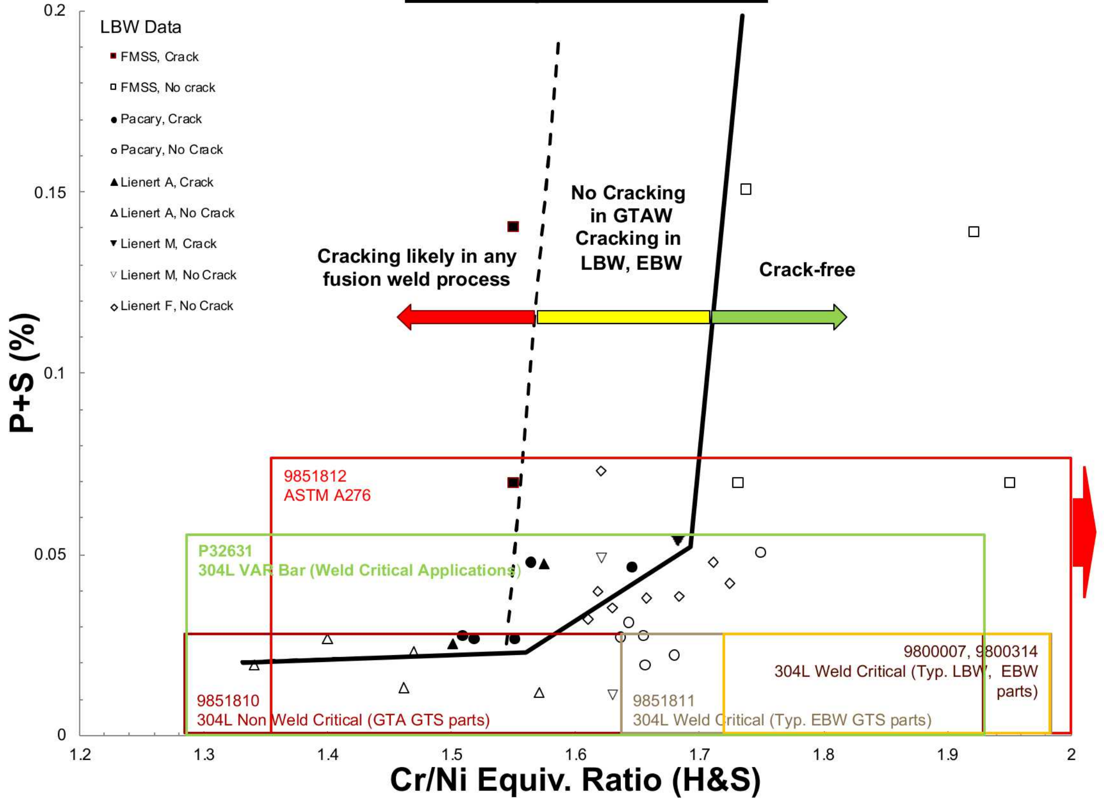

A brief history of boron in WC 304L

- Historically, boron was unspecified element. Impurity control focused on S and P.
- In 2011, incoming WC 304L VAR microstructure testing showed an unknown brown/gray phase coexisting with delta-ferrite stringers.
- This phase was eventually identified as a chromium-rich boride (M_2B)
- Composition measurements found the heat contained ~200 wt.ppm boron
- **A limit of 20 wt.ppm B limit was implemented to eliminate boride phase in future heats**

Electron Backscatter Diffraction (EBSD) patterns ID'ing boride phase

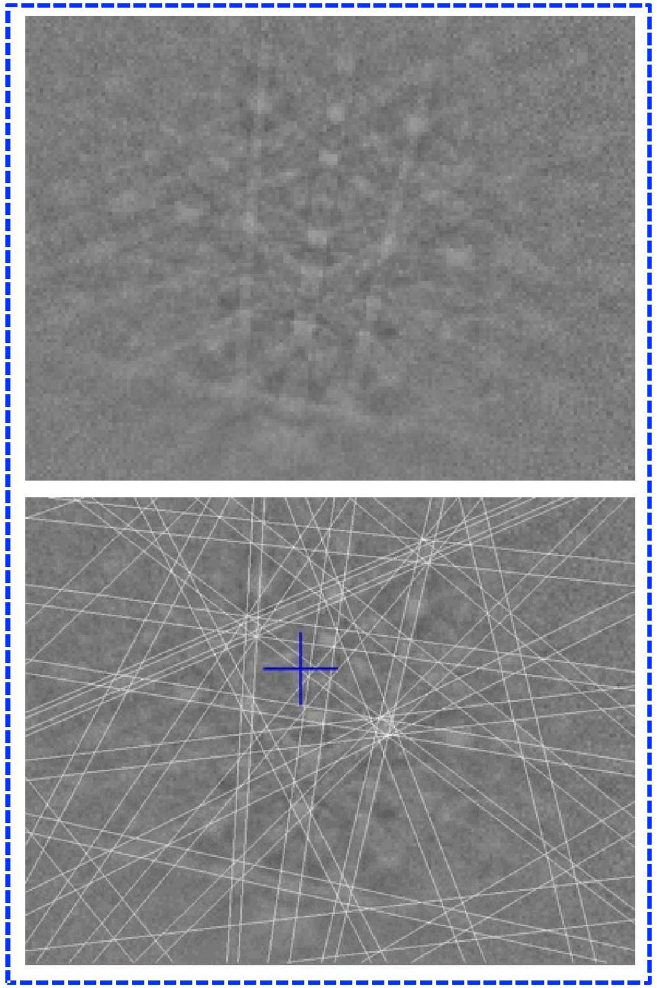

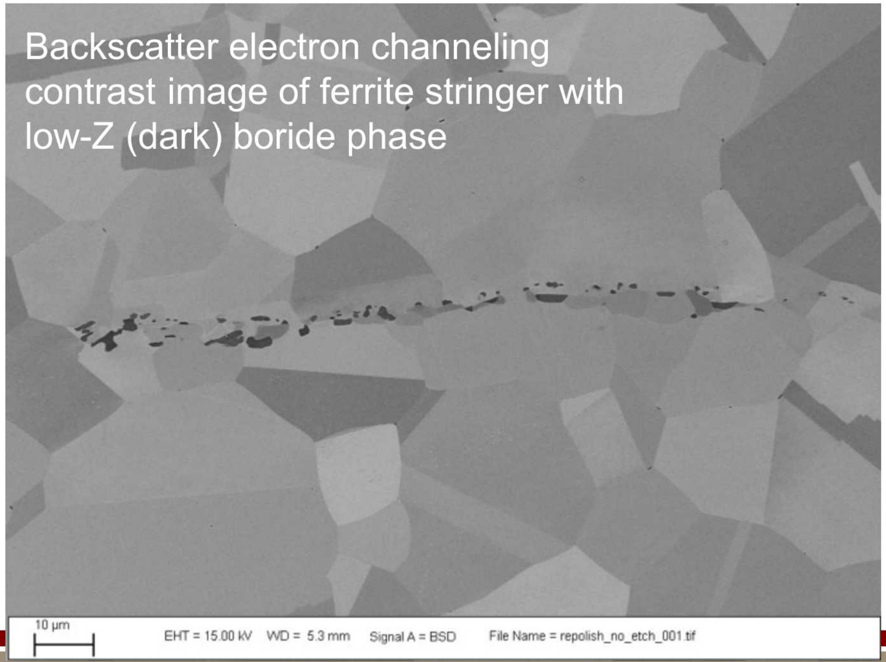

Backscatter electron channeling contrast image of ferrite stringer with low-Z (dark) boride phase

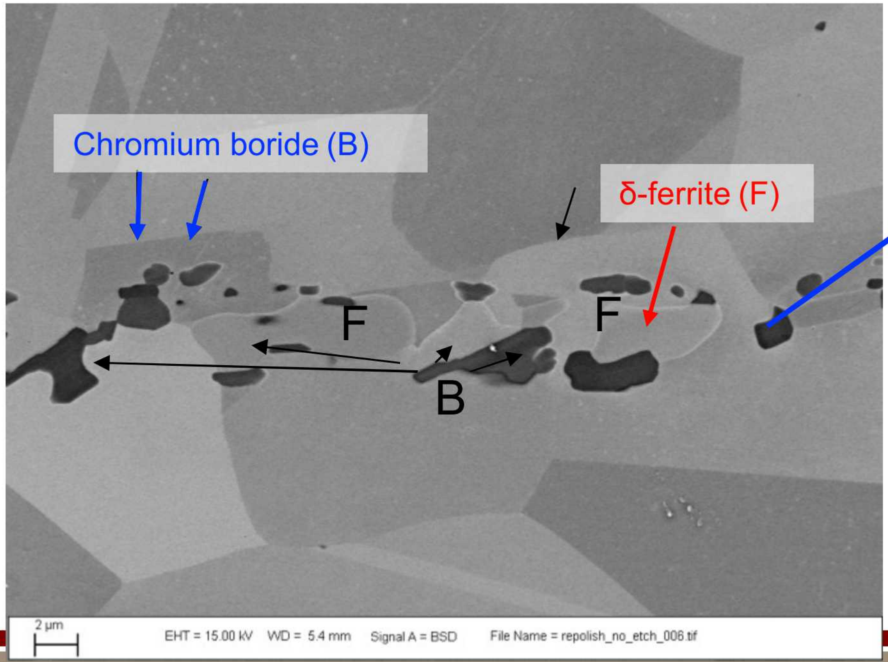

In 2016, chromium borides appear again in WC 304L

- Material made by different producer showed borides within ferrite stringers
- Alloy contained near the max. allowable B content of 20 wt.ppm due to intentional microalloying addition
- Additional characterization confirmed phase is boron-rich and structurally consistent with tetragonal M_2B
- **<u>Concerns raised with potential weldability issues related to the presence of borides</u>**

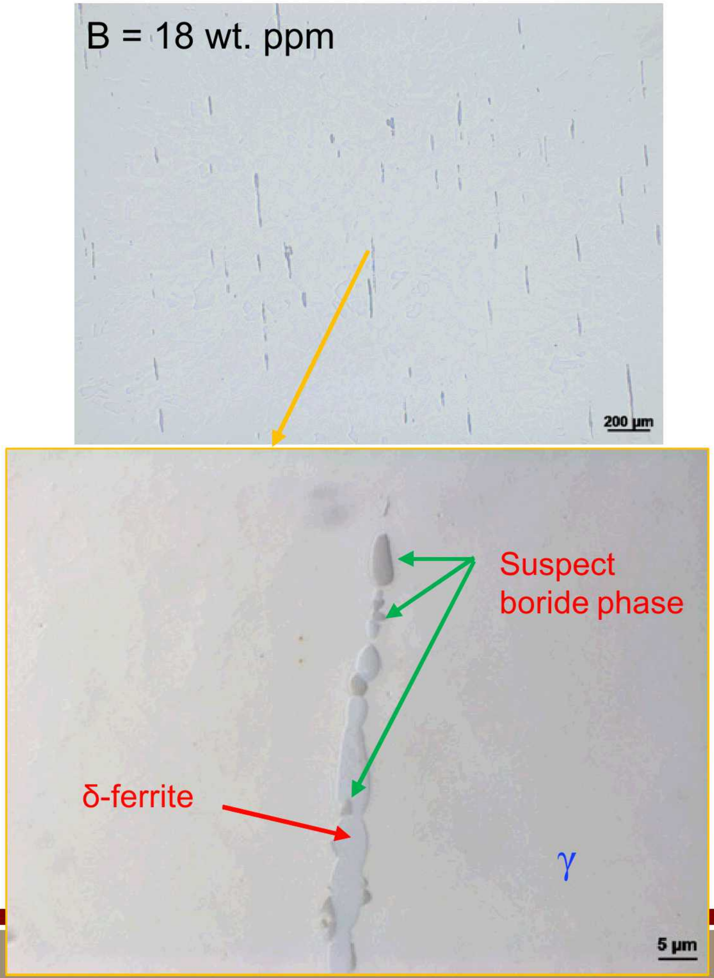

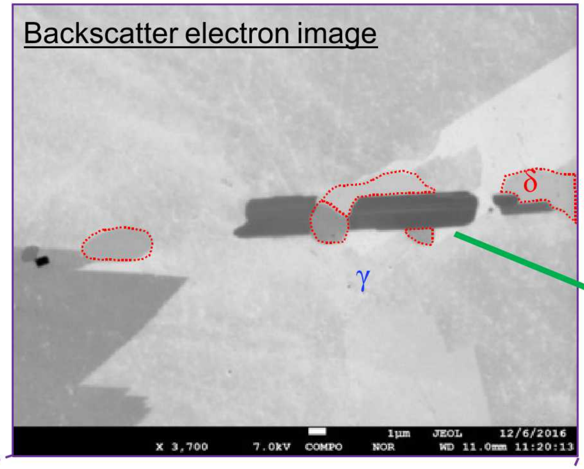

Wavelength Dispersive Spectroscopic Maps

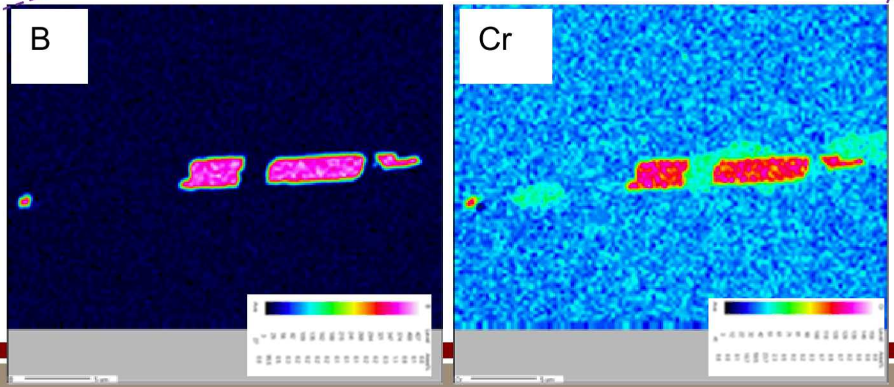

EBSD of Boride

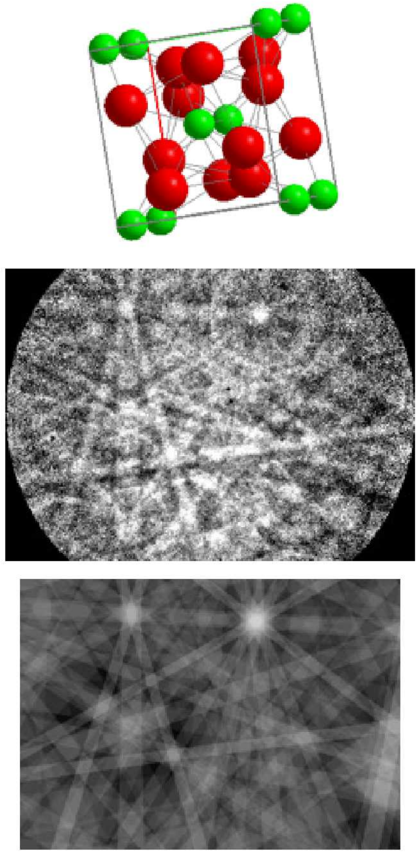

Kikuchi patterns index as tetragonal M_2B

Why are borides forming in WC 304L even at 20 wt.ppm B?

- The limit of 20 wt.ppm B was implemented based on quaternary phase equilibria data from Goldschmidt (1971).
- More recent multicomponent thermodynamic simulations performed at SNL show that solubility of boron in austenite during homogenization is closer to 5 wt.ppm!

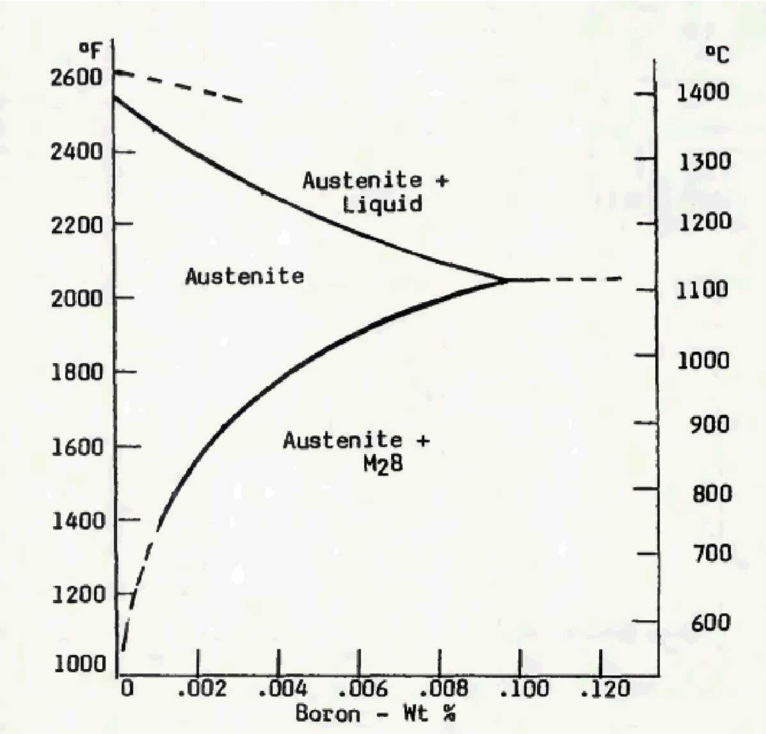

Solubility of B in Fe-18Cr-15Ni
(from Goldschmidt, 1971)

[Fe-X] – 19.19 Cr – 10.25 Ni – 0.024 C – X B , wt.%

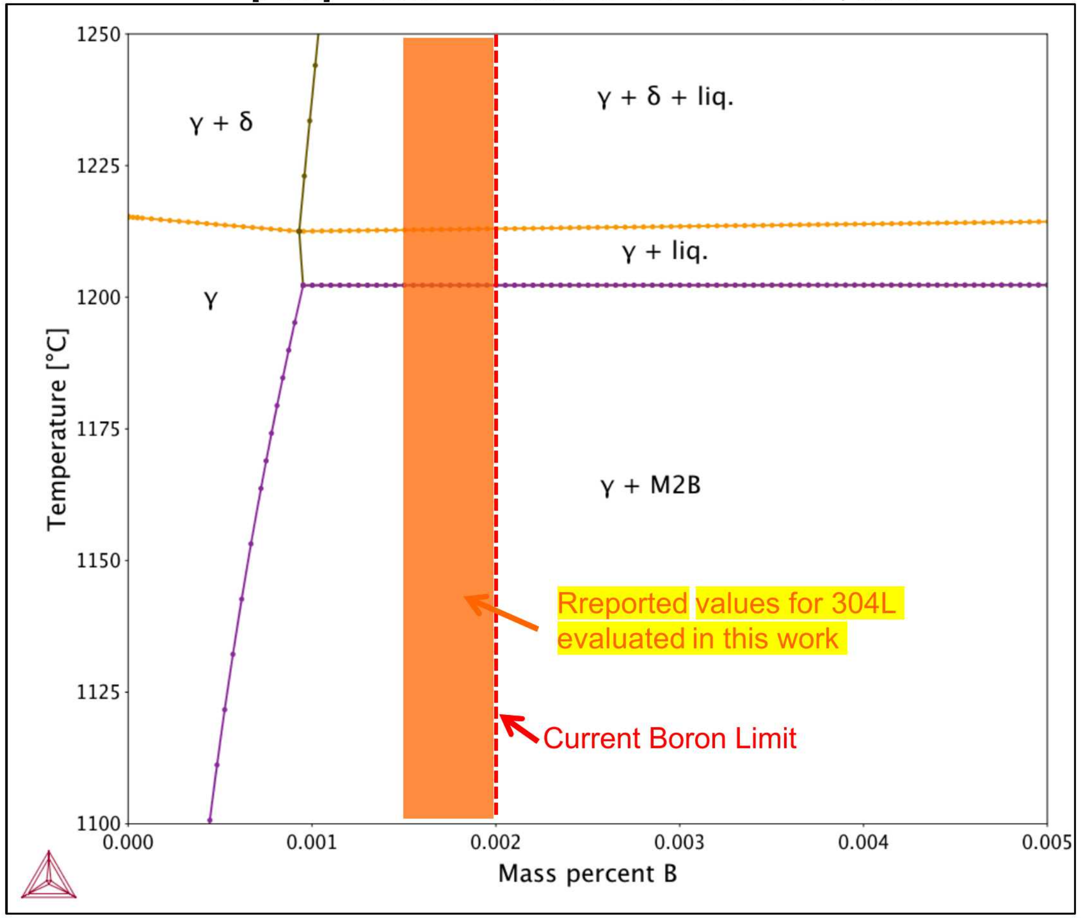

Gleeble hot ductility testing performed on 304L with varying boron content

- Only the highest boron content heat (340 wt.ppm B) shows markedly decreased hot ductility indicating HAZ cracking risk.
- For heats with <100 wt.ppm B., ductility recovers sharply on-cooling near the on-heating NDT

Custom 304L heats created with varying B content

Sample	304L - **19B** (VAR)	304L - **36B** (VIM)	304L - **96B** (VIM)	304L - **340B** (VIM)
		wt.%		
B	**0.0019**	**0.0036**	**0.0096**	**0.0340**
C	0.021	<0.001	<0.001	0.003
Cr	19.45	18.84	18.94	19.01
Cu	0.11	0.13	0.13	0.14
Mn	1.42	1.54	1.52	1.50
Mo	0.09	0.12	0.11	0.09
Ni	10.24	10.26	10.10	10.32
N	0.010	0.006	0.005	0.008
P	0.019	<0.005	<0.005	<0.005
Si	0.63	0.60	0.60	0.57
S	0.001	0.002	0.003	0.003
$Cr/Ni_{eq.}$*	**1.80**	**1.82**	**1.84**	**1.80**

Gleeble hot ductility signatures for B-containing 304L

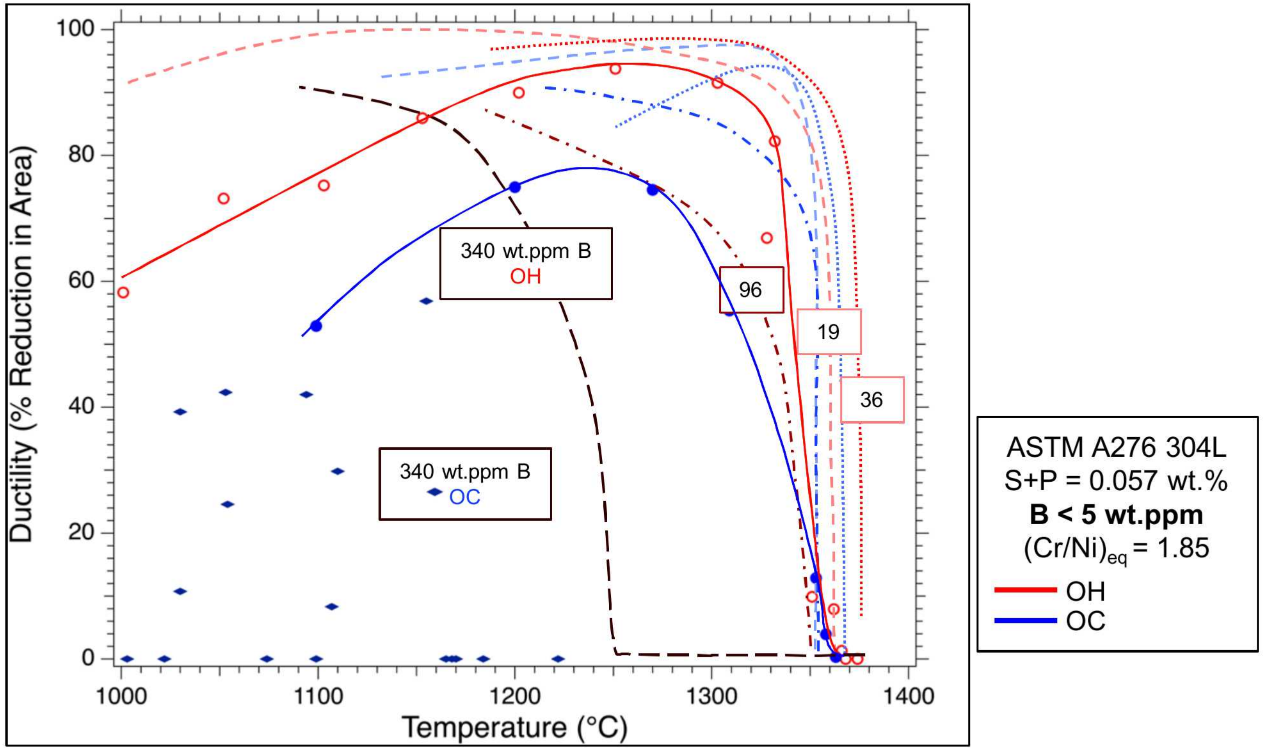

Autogenous welds showed differing HAZ cracking susceptibility for LBW vs. GTAW

- Testing showed no weldability issues for material at 20 wt.ppm B for both GTA and laser welds
    - Cracking in GTA HAZs was observed at 340 wt.ppm B material which is in good agreement with Gleeble Hot Ductility Testing
    - Laser welds showed considerably less margin with respect to cracking. HAZ cracks were observed at 36 wt.ppm associated with grain boundary borides

LBW

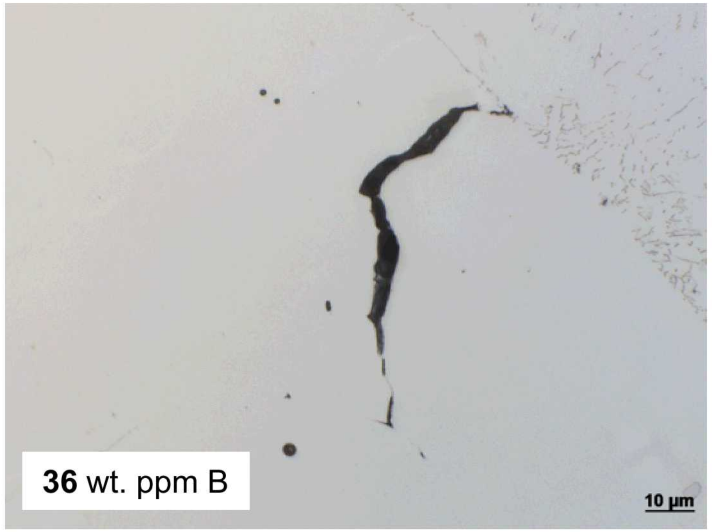

GTAW

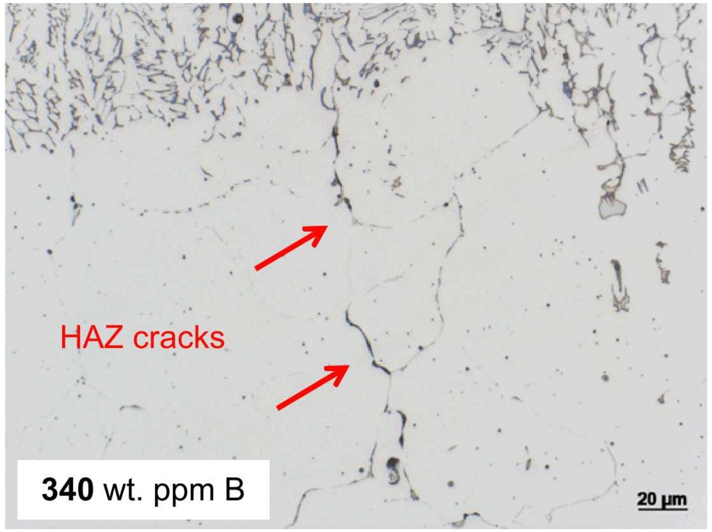

Crack tip

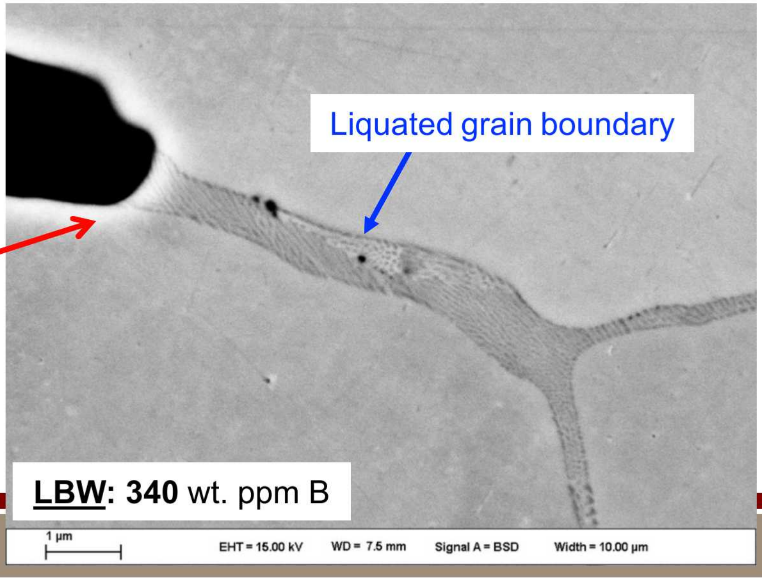

Path taken based on weldability testing

- Testing showed no weldability issues for material at 20 wt.ppm B for both GTA and laser welds
  - Cracking in GTA HAZs was observed at 340 wt.ppm B material which is in good agreement with Gleeble Hot Ductility Testing
  - Laser welds showed considerably less margin with respect to cracking. HAZ cracks were observed at 36 wt.ppm associated with liquated grain boundary borides

- Based on weldability data generated and known weld parameter space utilized in product end-use, this heat of WC304L VAR containing borides was eventually accepted

Anomalous HAZ cracking was observed on laser-welded WC 304L prototype parts

- Routine metallographic examination of laser welded hermetic prototype electrical feed-through assembly revealed HAZ cracks on part that underwent brazing. The braze was performed prior to welding
- Microstructural examination of brazed part showed unexpected intergranular phase formation. This phase was later determined to be boron-rich

Laser welds on WC 304L parts with ~20 wt.ppm B

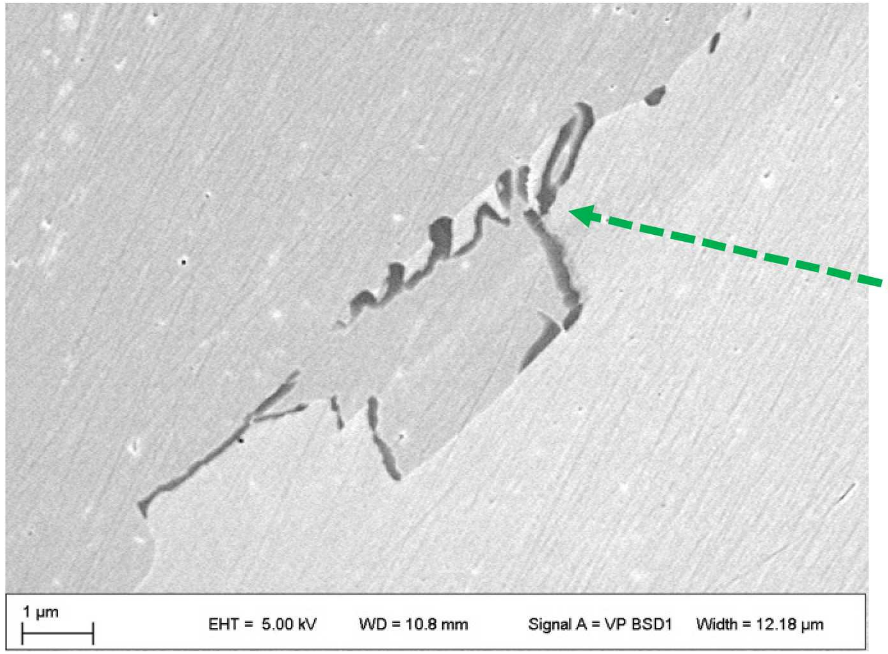

Low-Z intergranular boride phase. (ID'ed using TEM/EELS)

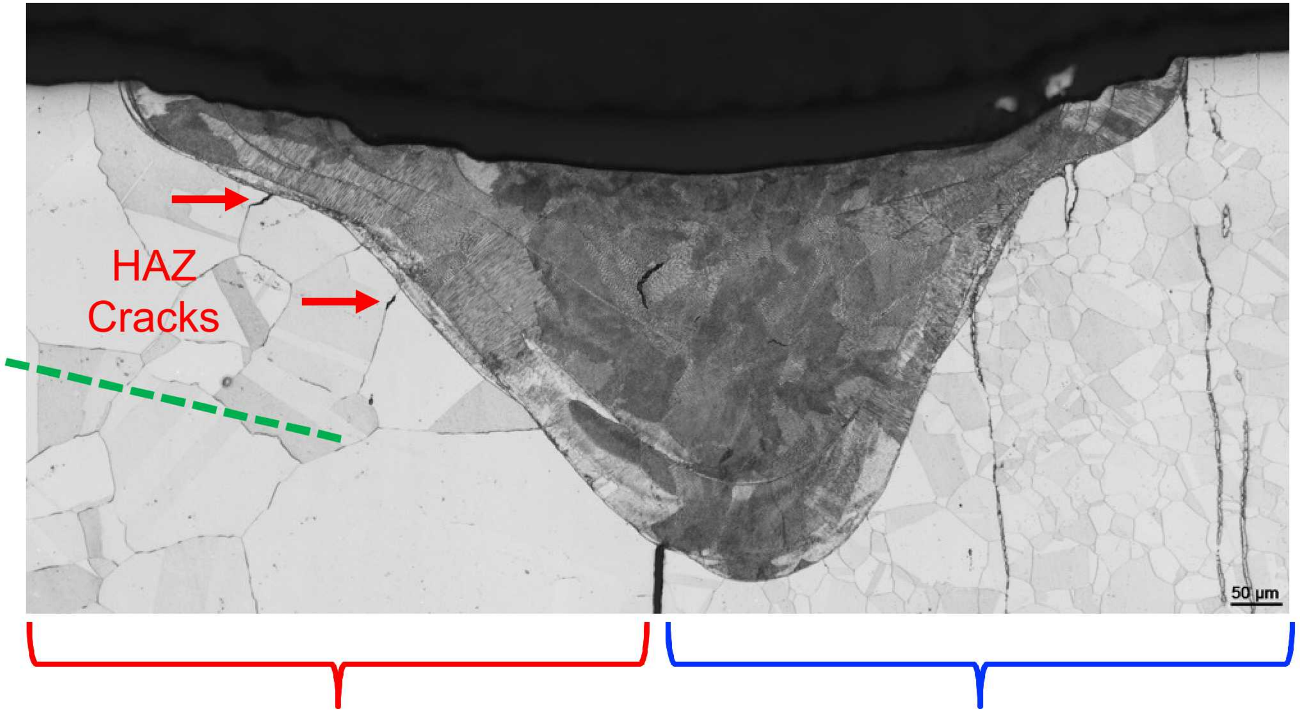

Brazed WC 304L part

WC 304L part (not brazed)

Thermal treatment alters boride distribution

- Exposure to elevated temperature can provide opportunity for boride to change morphology and distribution

1100°C, 1 hr.
(intergranular borides)

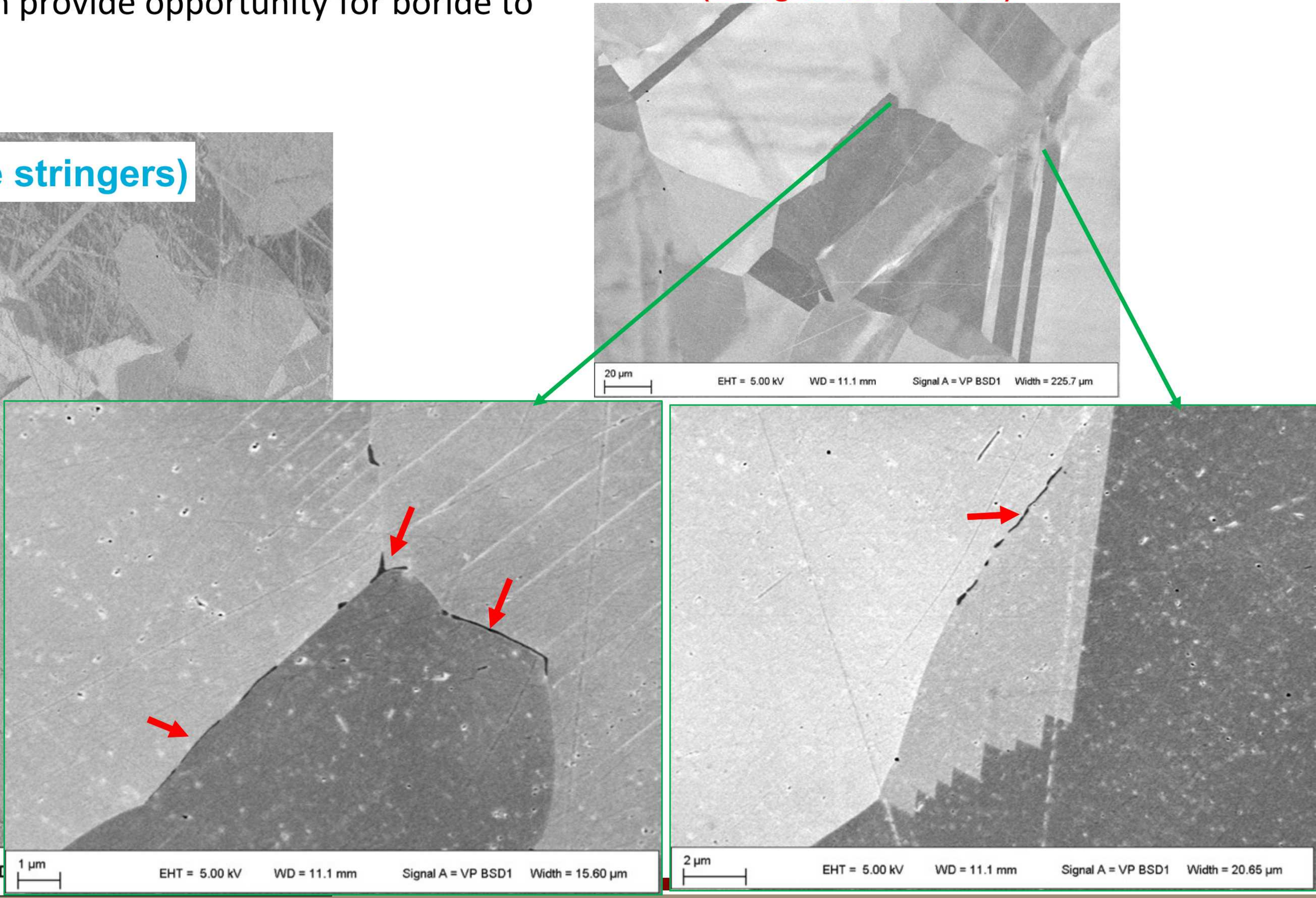

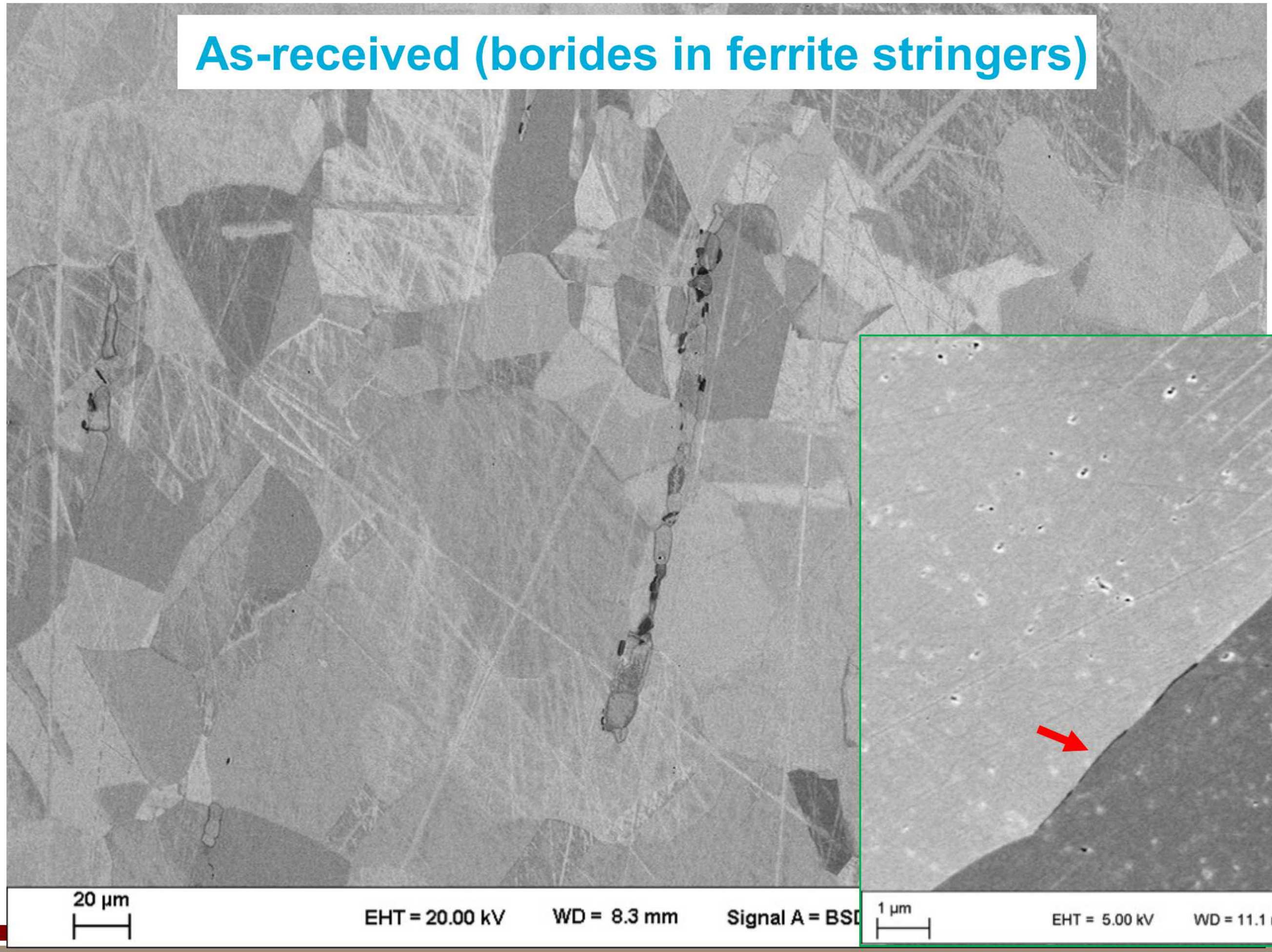

Detail: SEM Examination of HAZ Cracks

Pulsed Laser Seam Weld on WC 304L (~20 wt.ppm B) thermally treated 1100°C, 1 hr.

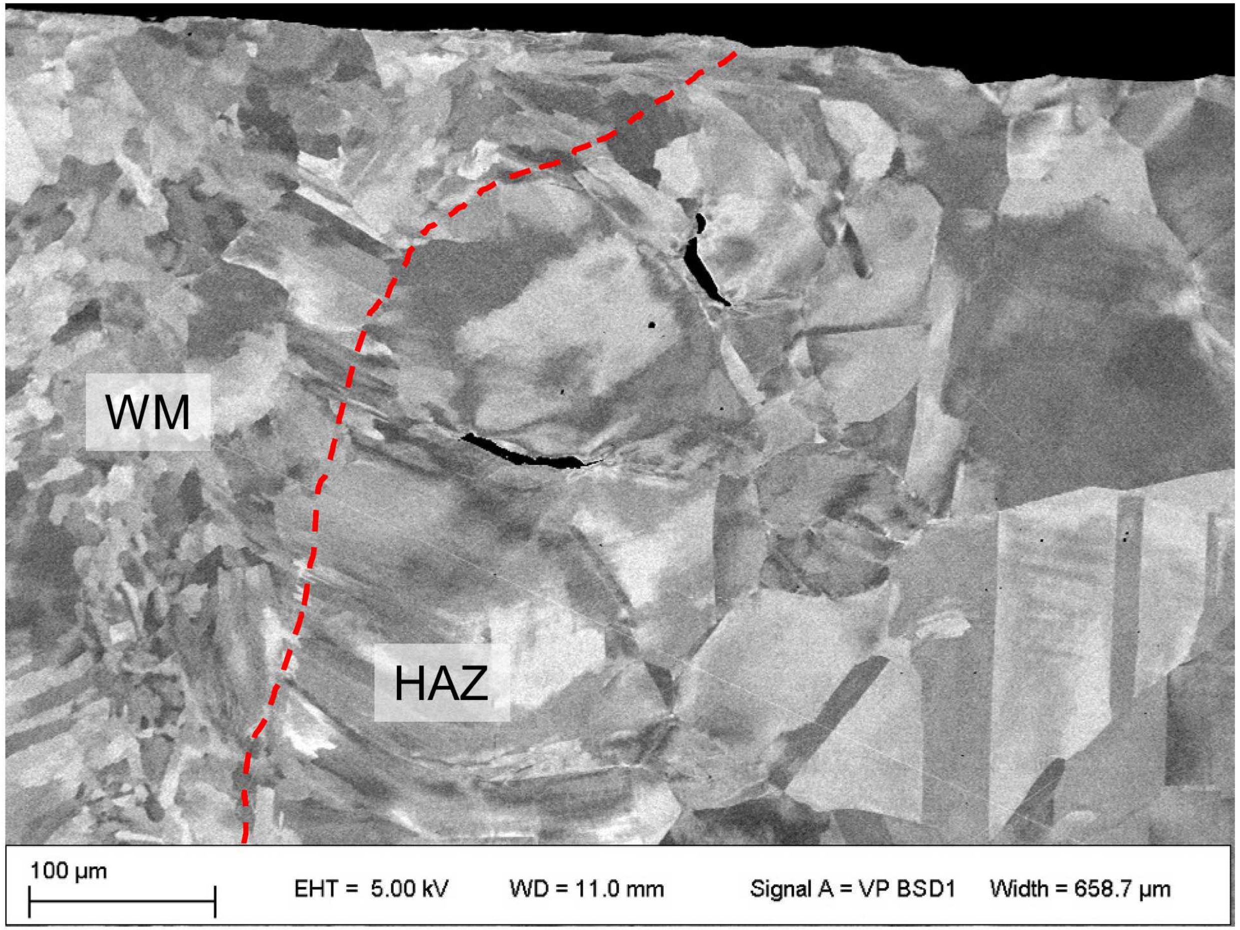

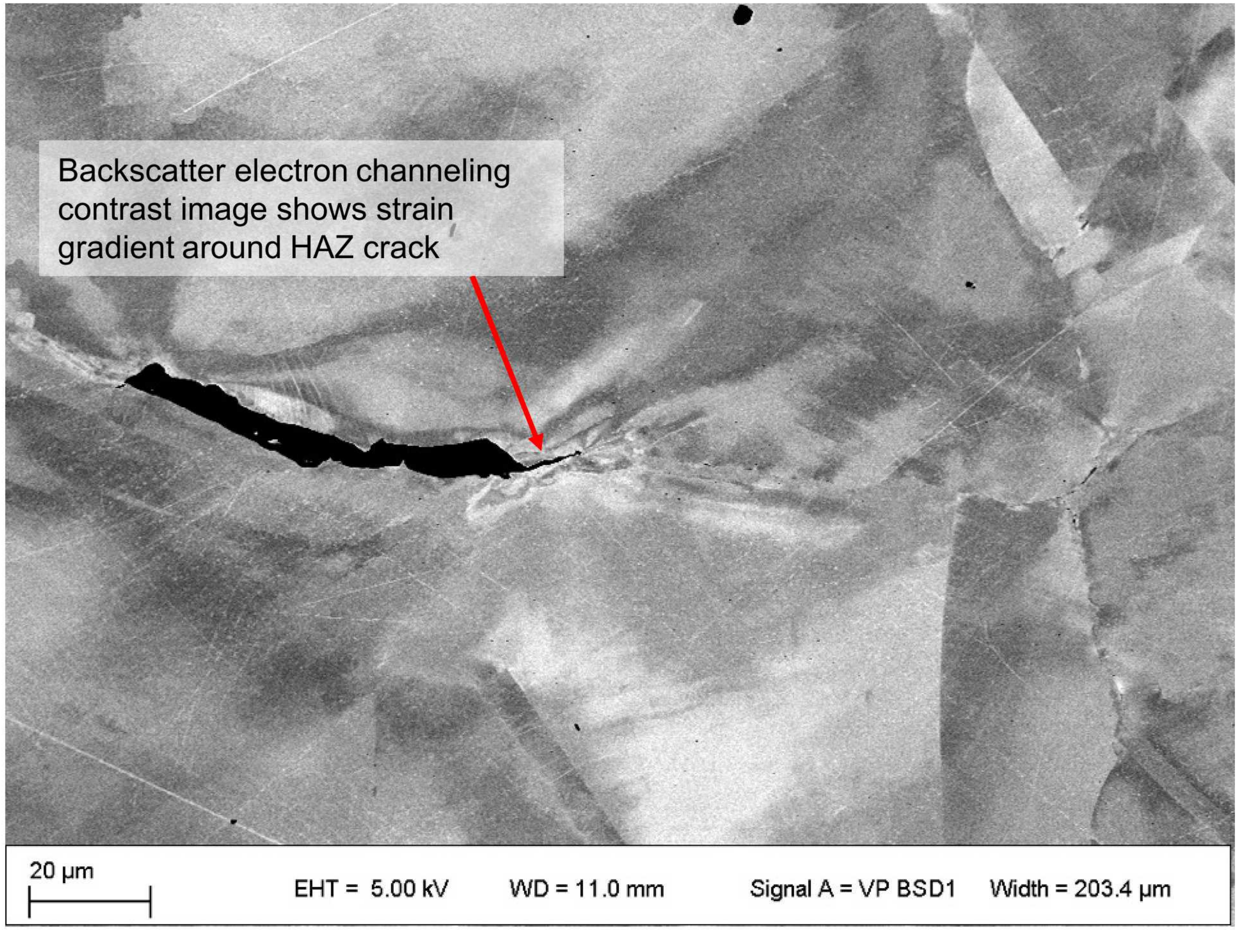

X-ray spectral imaging of intergranular phase

- Special energy dispersive spectroscopic analysis conditions provide qualitative map of boron concentration around HAZ grain boundaries

- Thermal treatment resulted in grain boundary boride film

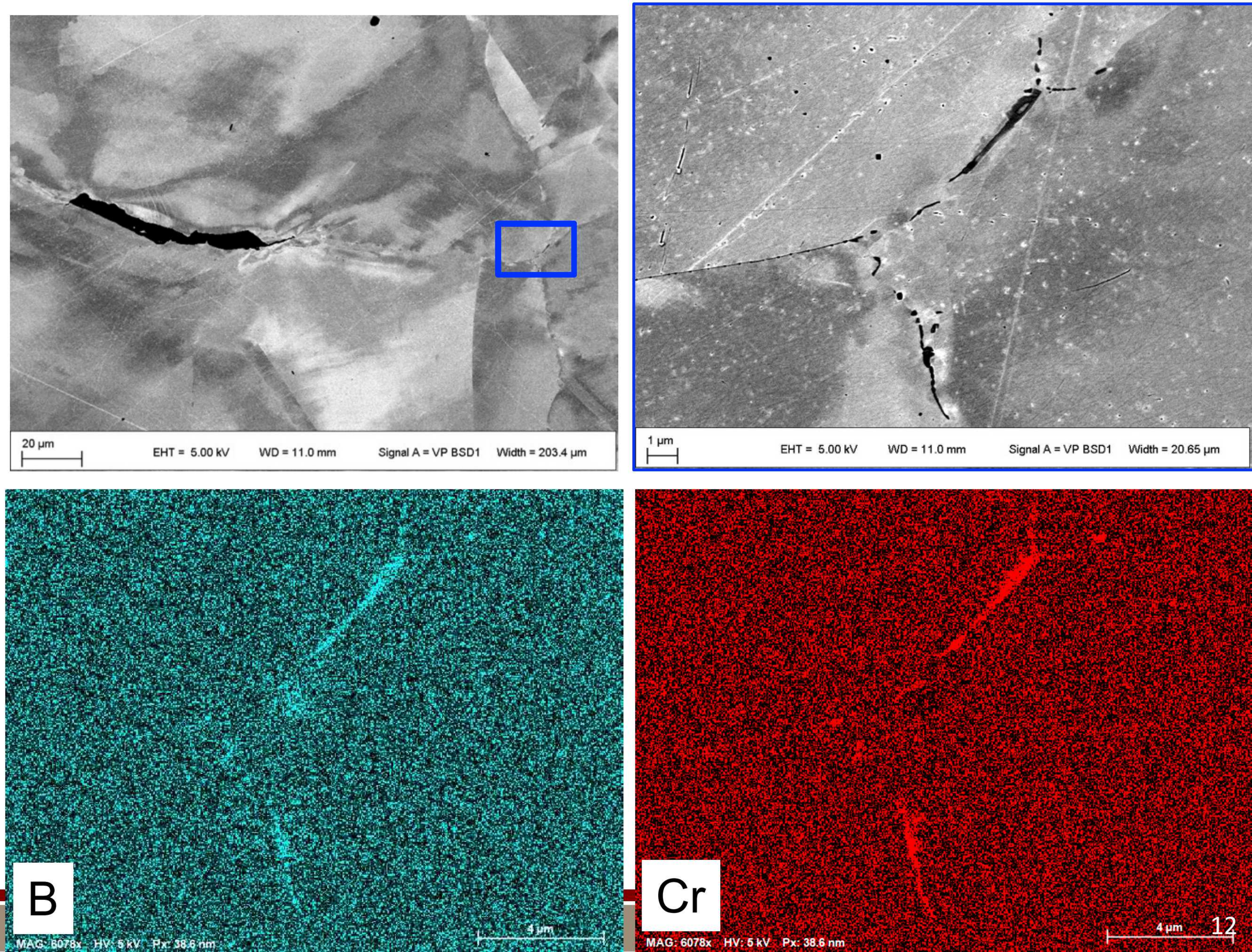

High temperature boride formation can make 304L HAZ liquation crack susceptible with thermal treatment

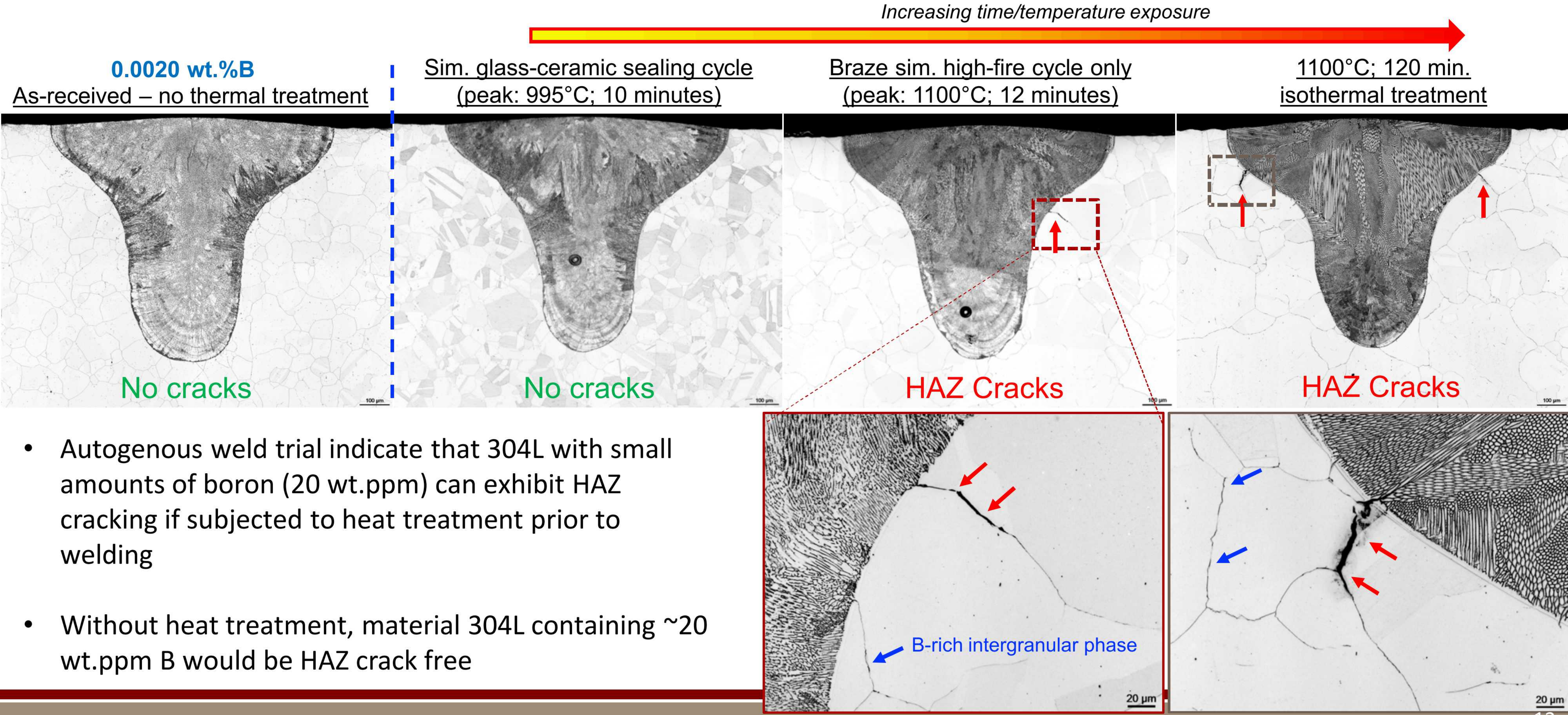

- Autogenous weld trial indicate that 304L with small amounts of boron (20 wt.ppm) can exhibit HAZ cracking if subjected to heat treatment prior to welding
- Without heat treatment, material 304L containing ~20 wt.ppm B would be HAZ crack free

HAZ cracking susceptibility depends on time-temperature history

- Continuing work to determine time-temperature dependence on weld HAZ crack susceptibility for boride-containing 304L

- Weld cracking risk for parts that undergo glass/glass-ceramic/brazing thermal cycles need to be evaluated on case-by-case basis due to vendor-specific high-temperature processing prior to hermetic sealing (e.g., ‘fire-off’ cleaning)

Autogenous laser weld trials

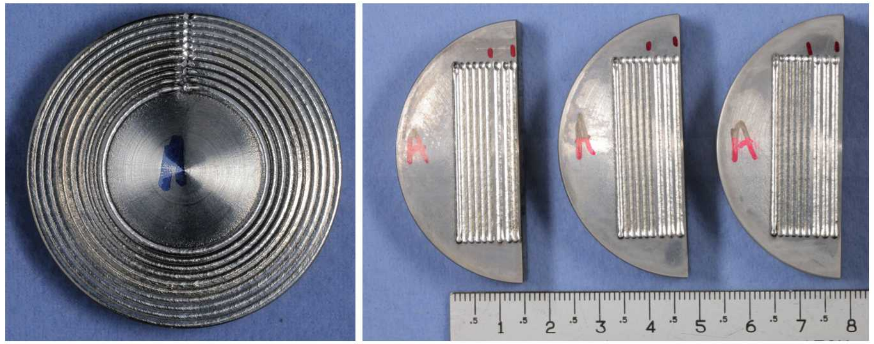

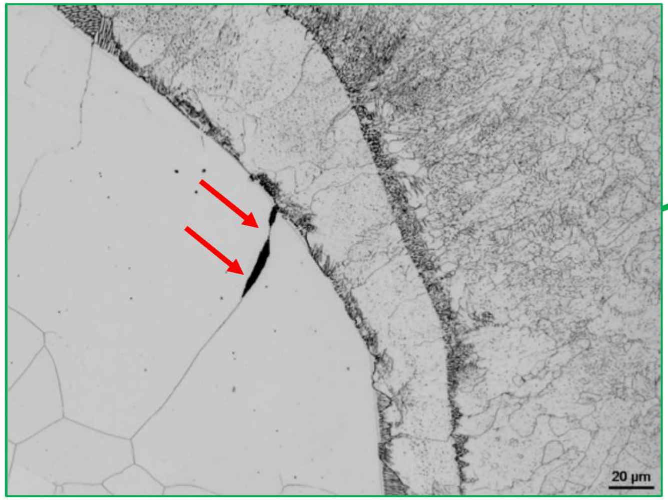

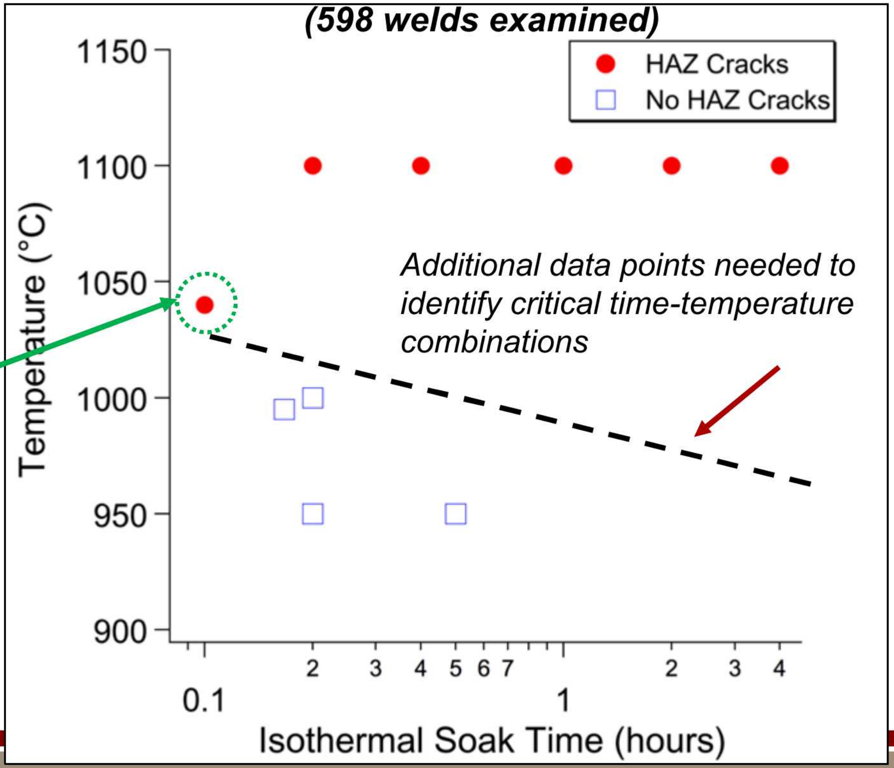

HAZ cracking susceptibility also depends on starting composition and microstructure

Cracking Response

 # welds with HAZ cracks / total # welds examined

- Two heats of WC 304L were subjected to various thermal cycles used for brazing
- Heats had similar boron concentration but differed in ferrite potential and starting ferrite content

2" dia. bar (half-round)
Low $(Cr/Ni)_{eq}$
20 wt.ppm B

4" dia. bar (quarter-round)
High $(Cr/Ni)_{eq}$
18 wt.ppm B

Fire-off (F-O) Cycle

Fire-off Run#**1**
950°C – 12 minutes

2" dia. bar	4" dia. bar
0 / 50	**0 / 50**

Fire-off Run#**2**
950°C – 30 minutes

2" dia. bar	4" dia. bar
0 / 50	**0 / 50**

Fire-off Run#**3**
1000°C – 12 minutes

2" dia. bar	4" dia. bar
0 / 50	**0 / 50**

Fire-off Run#**4**
970°C/20 min + 1040°C/5 min

2" dia. bar	4" dia. bar
2 / 50	**0 / 50**

+ Braze (850°C Peak)

F-O #1 + Braze

2" dia. bar	4" dia. bar
0 / 50	**0 / 50**

F-O #2 + Braze

2" dia. bar	4" dia. bar
0 / 50	**0 / 50**

F-O #3 + Braze

2" dia. bar	4" dia. bar
0 / 50	**0 / 50**

F-O #4 + Braze

2" dia. bar	4" dia. bar
1 / 50	**0 / 50**

Detail micrographs: F-O #4 *(970C/20 min + 1040C/5 min)*

Effect of alloy ferrite potential

- $(Cr/Ni)_{eq}$ ratio is generally used as a predictor of weld solidification mode; however, it can also be a measure of ferrite stability in 304L. Ratio is directly proportional to ferrite potential.
- HAZ liquation cracking susceptible microstructure appears to be predicated on complete dissolution of ferrite stringers during heat treatment
  - Elimination of ferrite stringers promotes larger grain size and formation of intergranular borides—both factors increase HAZ liquation crack susceptibility

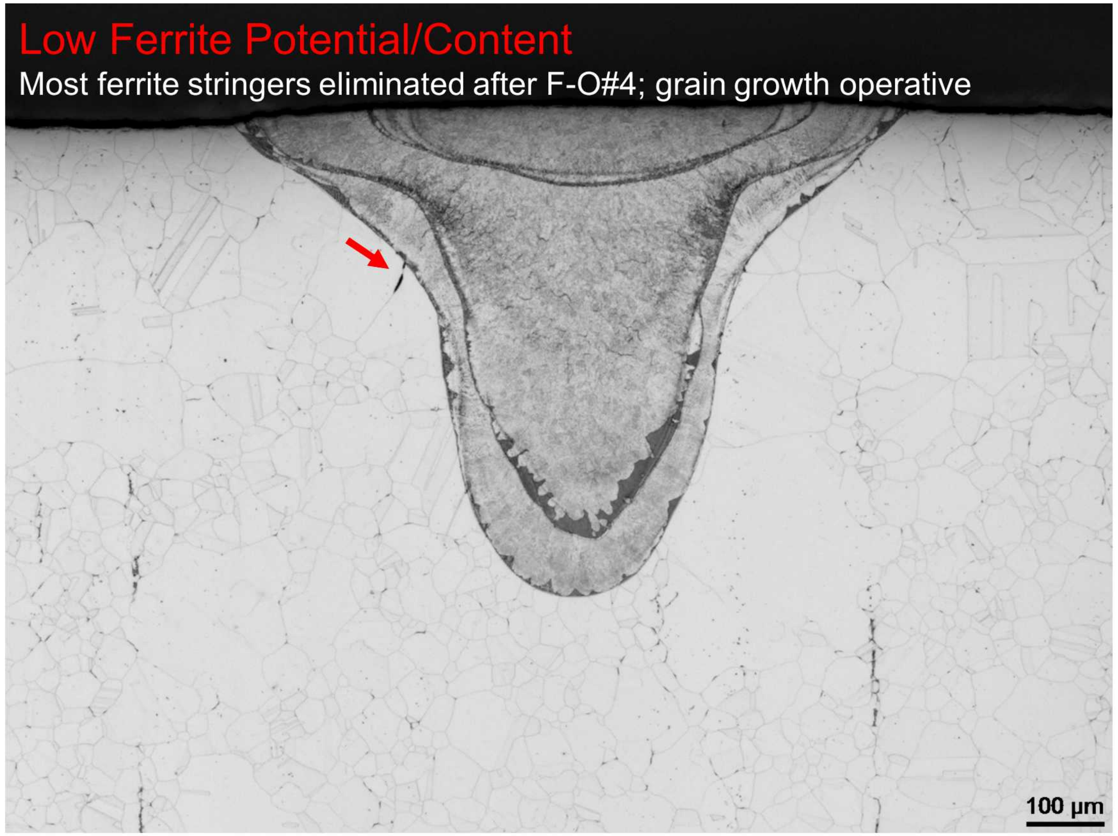

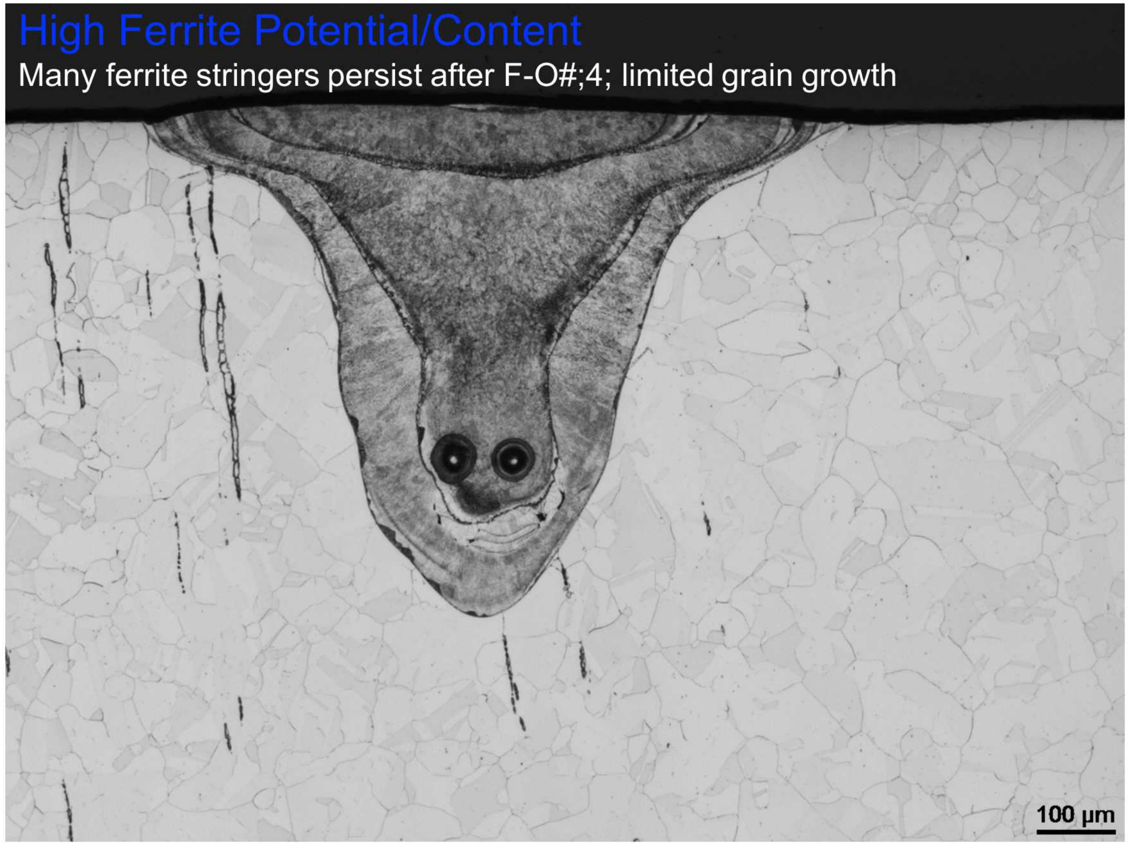

Detail micrographs

Most severe condition: F-O#4 + Braze + Re-braze

- Cumulative thermal history of samples metallographically evaluated does not results in microstructural changes to 304L VAR that result in HAZ liquation cracking

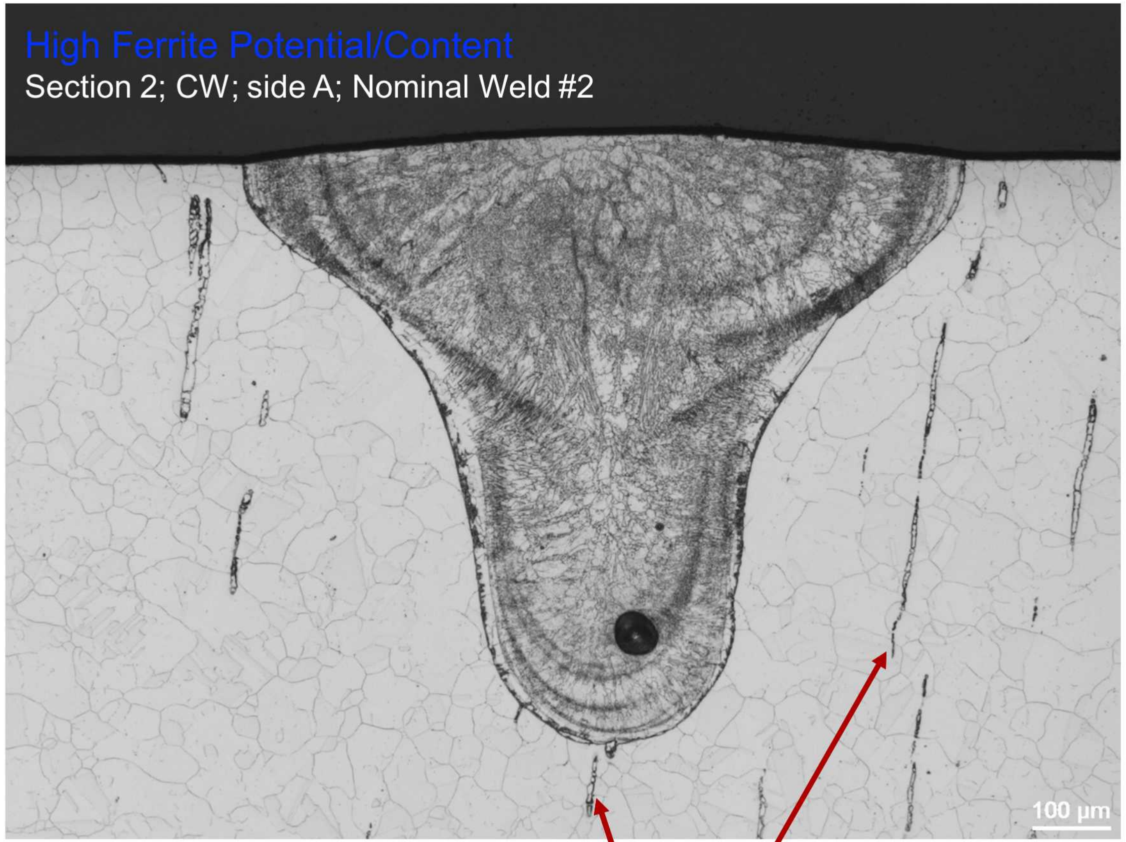

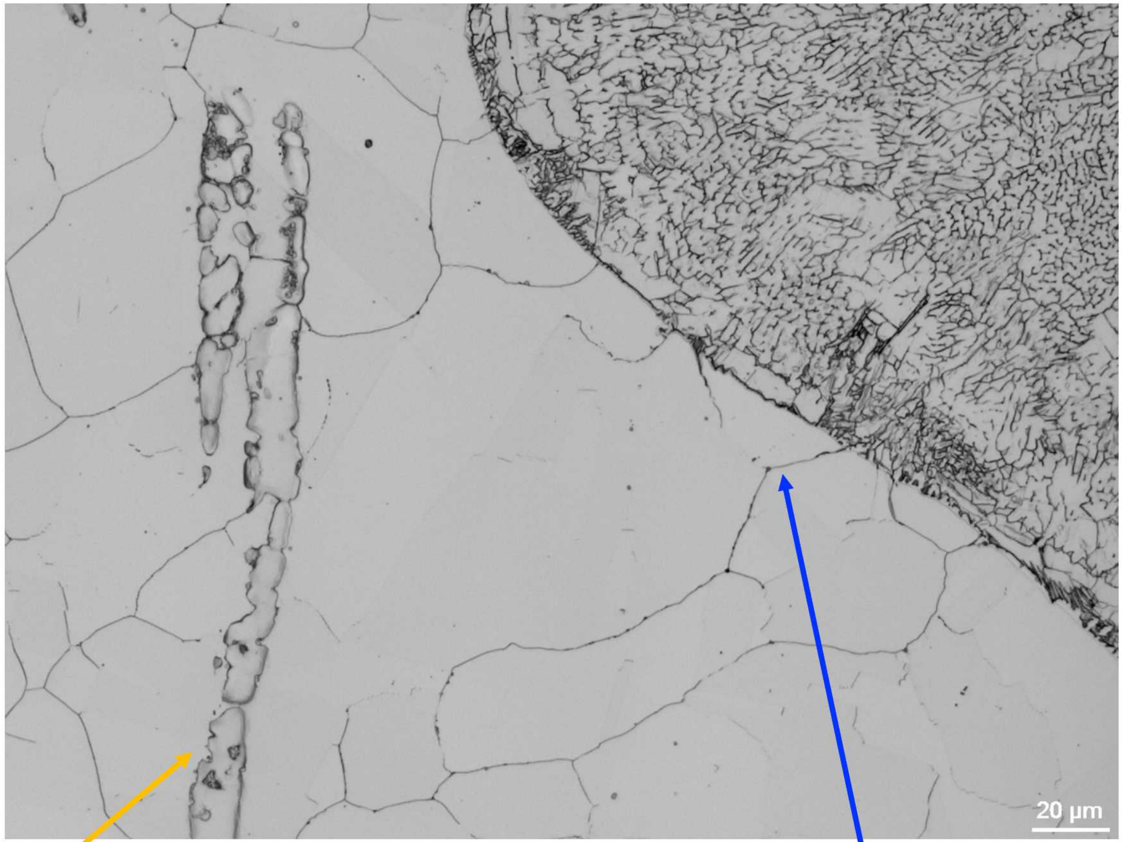

Ferrite+boride stringers largely persist after heat treatment

Serrated ferrite/austenite phase boundary suggests some operative dissolution operative as a result of heat treatment; however, complete dissolution of stringer did not occur

Limited intergranular boride formation

HAZ liquation cracks found in low ferrite potential 304L material if subjected to high-temperature fire-off cycle (F-O-#4)

- Highest peak temperature (1040C) of F-O#4 thermal cycle resulted in microstructural changes that led to HAZ liquation cracking susceptibility
  - Ferrite+boride stringer dissolution + grain growth + intergranular Cr_2B formation
- No HAZ cracks found in any other conditions with lower peak temperatures (F-O#1 – F-O#3) for this heat

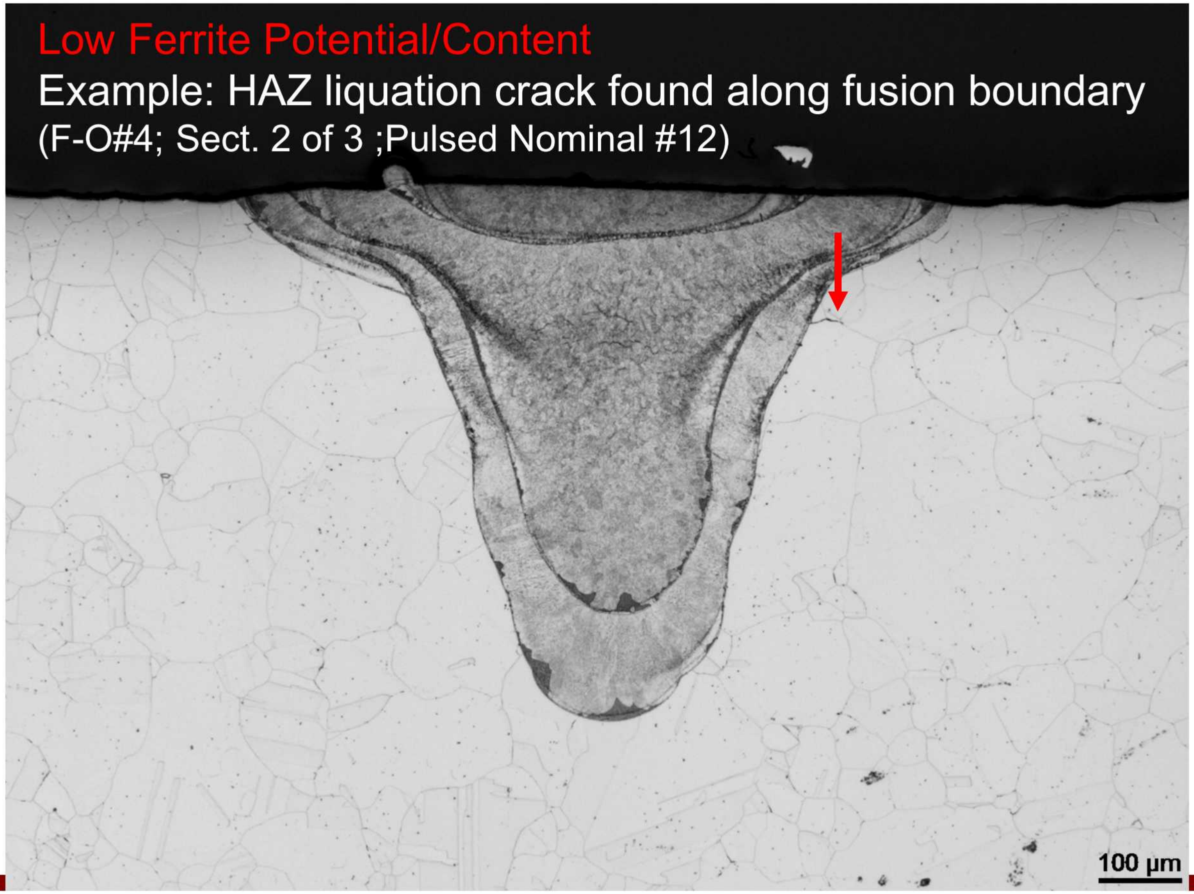

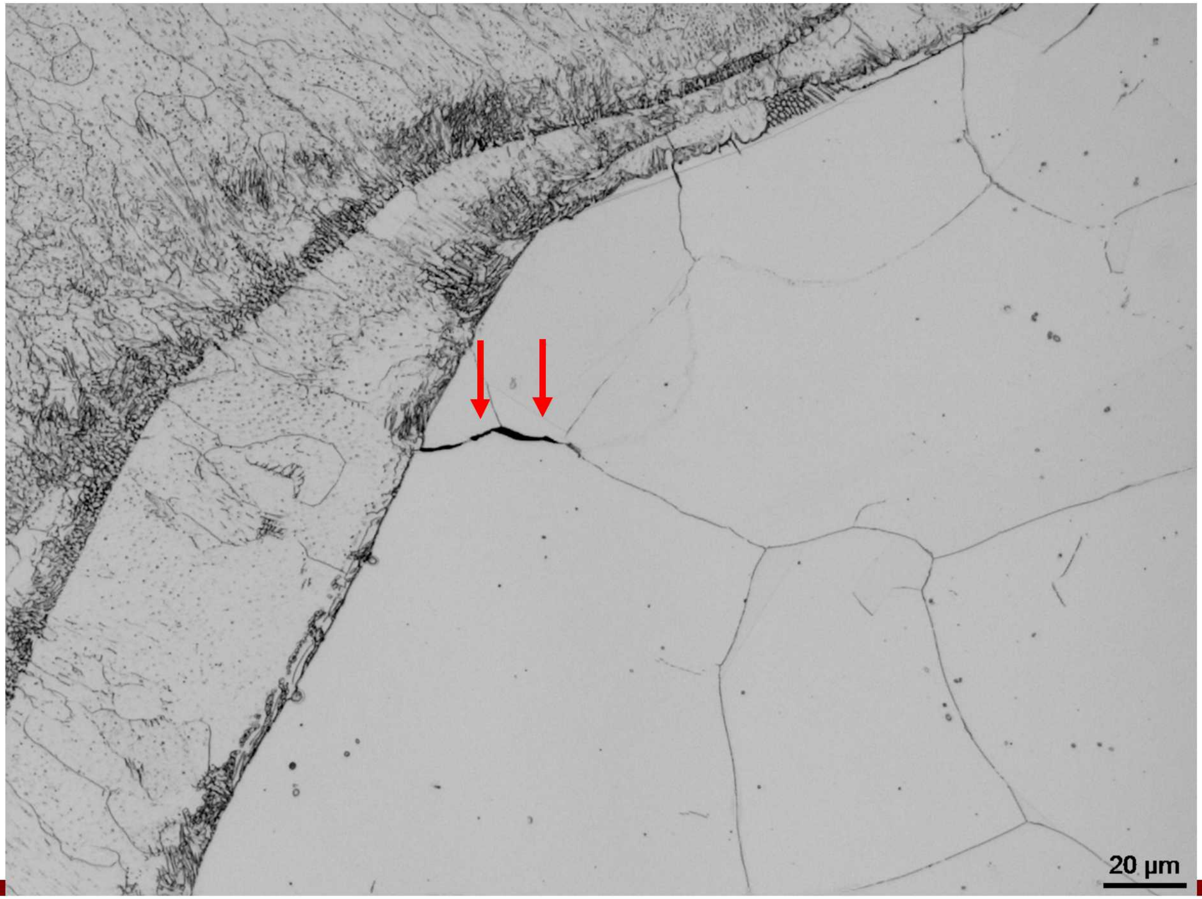

Concluding Remarks

- If WC 304L is not thermally processed, boron concentrations up to ~20 wt.ppm B do not result in HAZ liquation cracking issues based on autogenous welds and HAZ thermophysical simulation

- Additional thermal processing of WC 304L can result in demonstrated HAZ crack susceptibility for a material that would otherwise be immune to HAZ cracking. Materials with specification-compliant B concentrations can be crack susceptible if thermally treated above 1000C

- HAZ cracking in thermally processed 304L appears to be associated with dissolution of ferrite/chromium boride stringers with grain growth
  - Increased boron concentration at the grain boundaries can lead to Cr_2B formation/liquation and/or incipient melting. More detailed microstructural examination is planned.

- Specification requirements for WC 304L VAR are continually evolving to take into account manufacturing trends. Changes are being implemented to lower limit to <5 wt.ppm B to circumvent HAZ cracking risk for material subject to thermal processing

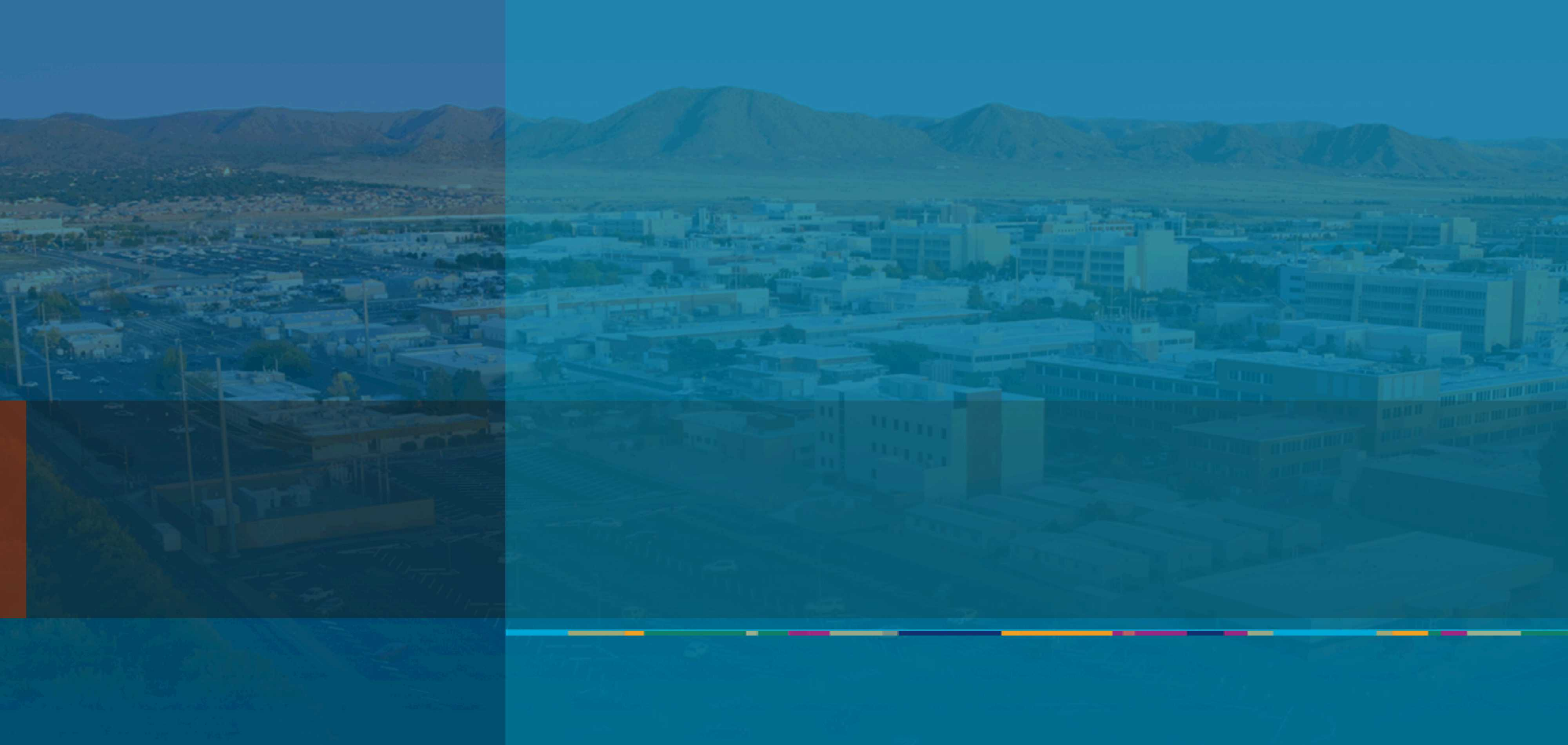

Controlled-B 304L heats produced to study micro-alloying effects on weldability

- Boron content from 19 to 340 wt.ppm examined
- Small (20 lb.) vacuum induction melted (VIM) heats produced with compositions targeted to be similar to heat originally observed containing Cr_2B
- All alloys examined have low S + P impurity levels combined with high $(Cr/Ni)_{eq}$ ratios expected to solidify as primary ferrite during laser welding

Grain boundary B segregation in 316L with **40 wt.ppm B**[1]

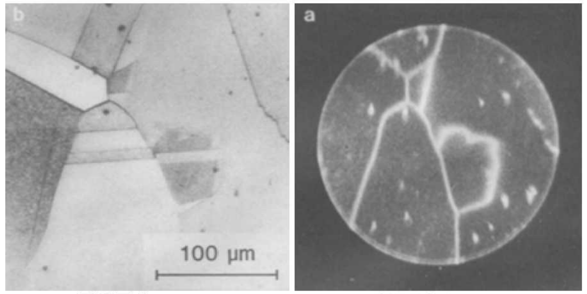

BSE Image SIMS Image

Creep-life enhanced 308 filler metal[2]

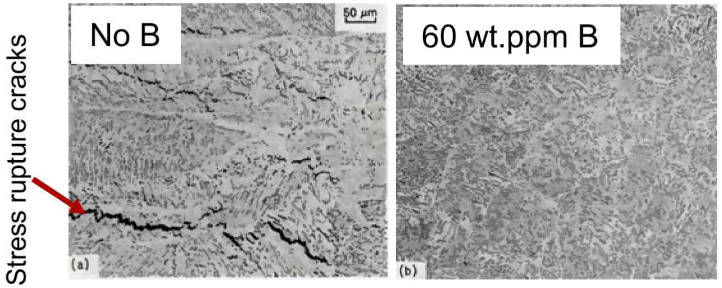

Sample	304L - **19B** (VAR)	304L - **36B** (VIM)	304L - **96B** (VIM)	304L - **340B** (VIM)
		wt.%		
B	**0.0019**	**0.0036**	**0.0096**	**0.0340**
C	0.021	<0.001	<0.001	0.003
Cr	19.45	18.84	18.94	19.01
Cu	0.11	0.13	0.13	0.14
Mn	1.42	1.54	1.52	1.50
Mo	0.09	0.12	0.11	0.09
Ni	10.24	10.26	10.10	10.32
N	0.010	0.006	0.005	0.008
P	0.019	<0.005	<0.005	<0.005
Si	0.63	0.60	0.60	0.57
S	0.001	0.002	0.003	0.003
$Cr/Ni_{eq.}$ *	**1.80**	**1.82**	**1.84**	**1.80**

Production-scale melt hot worked into 4" bar

~20 lb. VIM 304L ingots. Ingots hot rolled into 1" bar, annealed 1100°C/1hr.

1. Karlsson, L., et al. Acta Metall. Vol. 36, No.1, 1-12, 1988
2. Kleuth, R.L., et a., Welding Journal, 65, 1s-7s, 1986

*O. Hammar and U. Svennson, Solidification and Casting of Metals, Metal Society, London 1979.
$(CrNi)_{eq}$ = [Cr+1.37(Mo)+1.5(Si)+2.0(Nb)+3.0(Ti)] / [Ni+0.31(Mn)+22(C)+14.2(N)+Cu]

Assessing Weld HAZ susceptibility: Approach

- Assessing boron micro-alloying effects on HAZ liquation cracking susceptibility will utilize both simulative weldability testing and autogenous weld trials

#1:
Evaluation of elevated temperature ductility

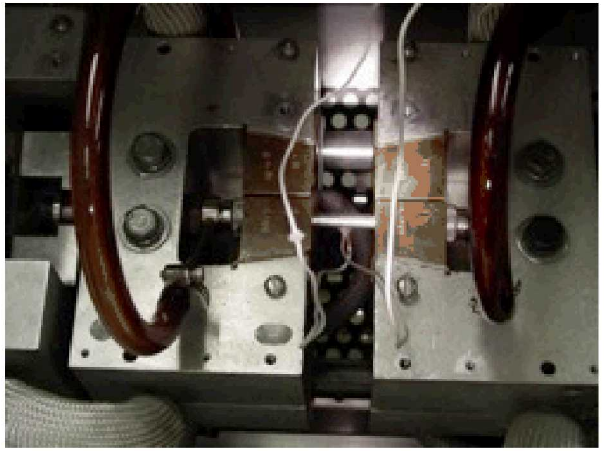

Gleeble Thermomechanical Simulator

#2:
Autogenous GTA and laser welds

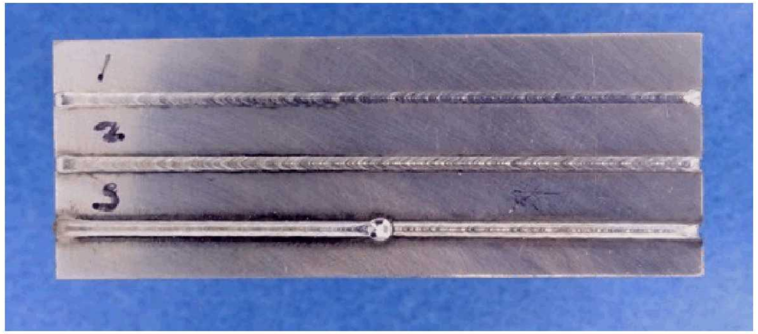

Gleeble Hot Ductility Test

- High-temperature ductility response of material provides insight into material weldability
- HAZ cracking generally associated with exhaustion of available ductility

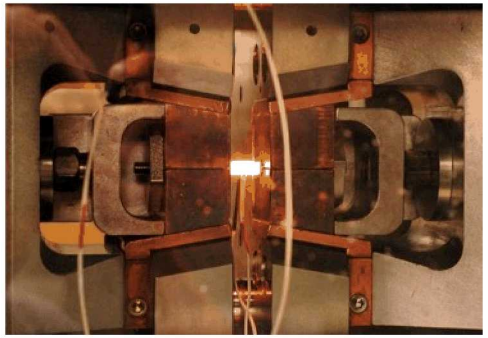

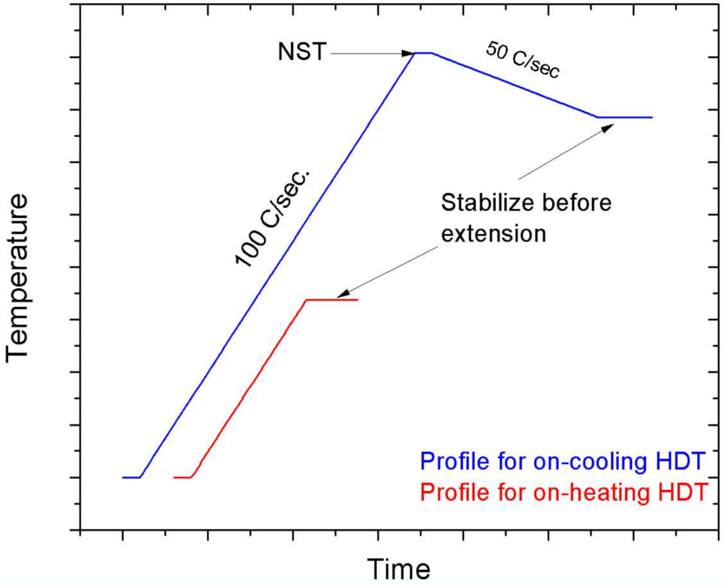

Schematic of Hot Ductility Signature

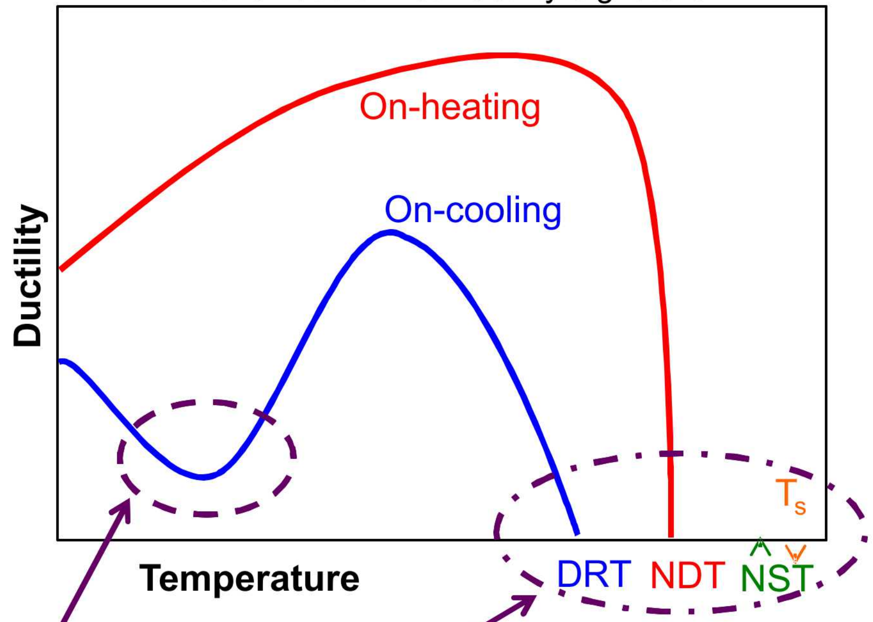

Insight into sub-solidus crack susceptibility

Insight into liquation crack susceptibility

NST: Nil-strength temperature
NDT: Nil-ductility temperature
DRT: Ductility recovery temperature

Translation of Measured HDT Temperatures to HAZ Crack Susceptible Regions (CSR)

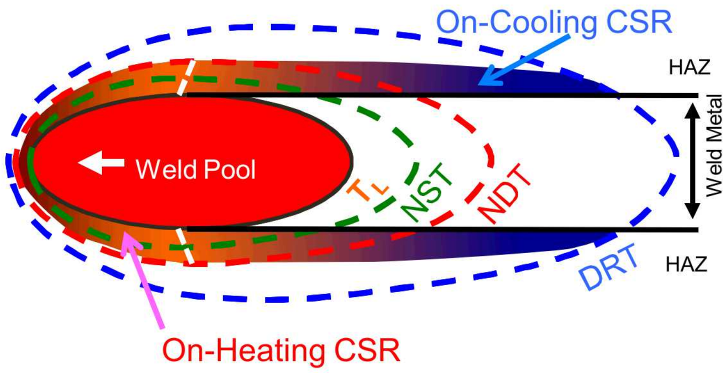

On-heating ductility signature

- Ductility decreases precipitously for B contents ≤ 96 wt. ppm around 1350°C; with the 96 wt.ppm B condition exhibiting a wider temperature range over which ductility decreases
- Highest B condition (340 wt.ppm) demonstrated nil-ductility temperature (NDT) approximately 100°C lower than other conditions

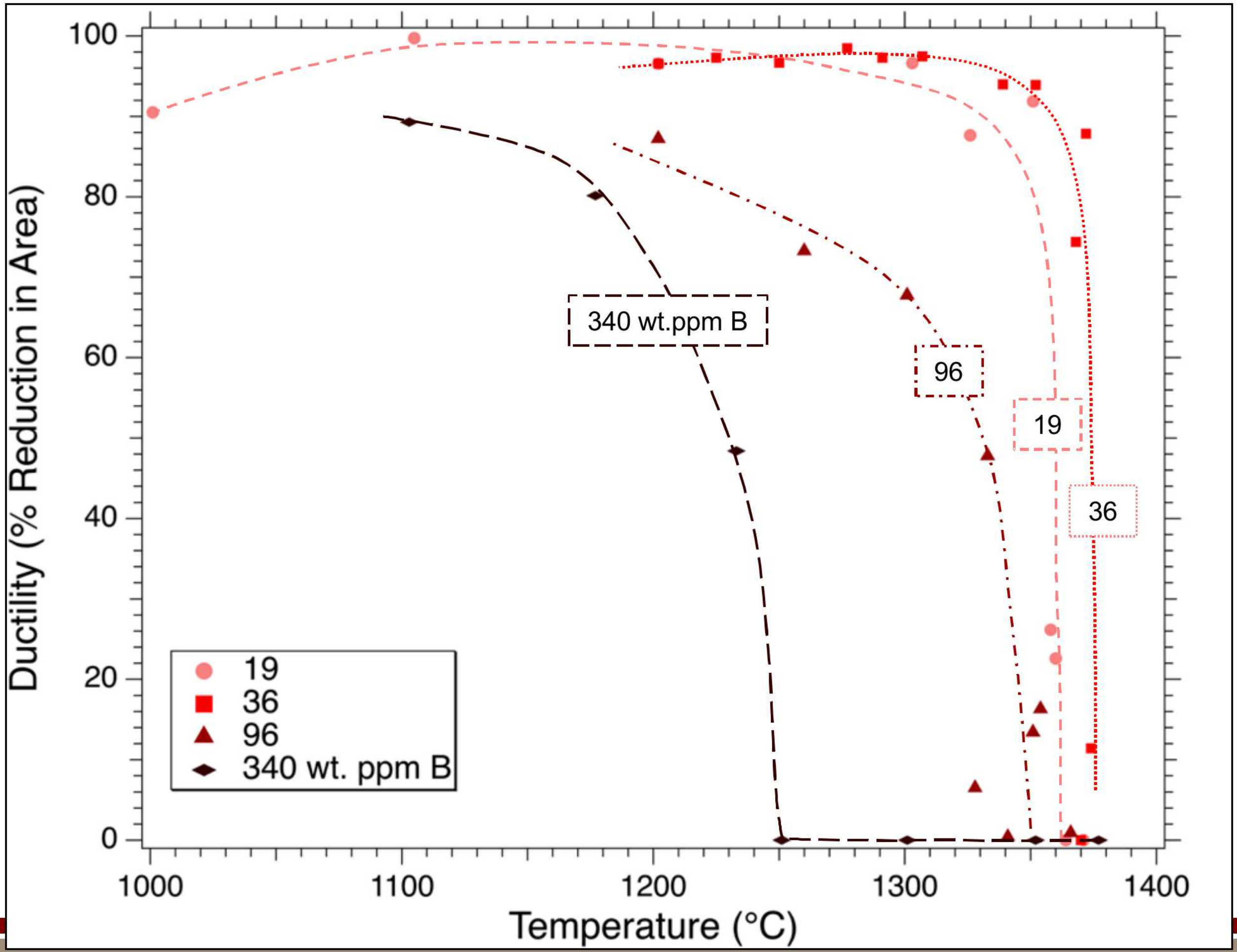

On-cooling ductility signature

- 19, 36, and 96 wt.ppm B specimens exhibited rapid ductility recovery on-cooling
- 340 wt.ppm B condition exhibits ductility recovery 200+°C lower than other conditions evaluated
- Longitudinal cross sections near fracture for 340 ppm needed to better understand ductility variability

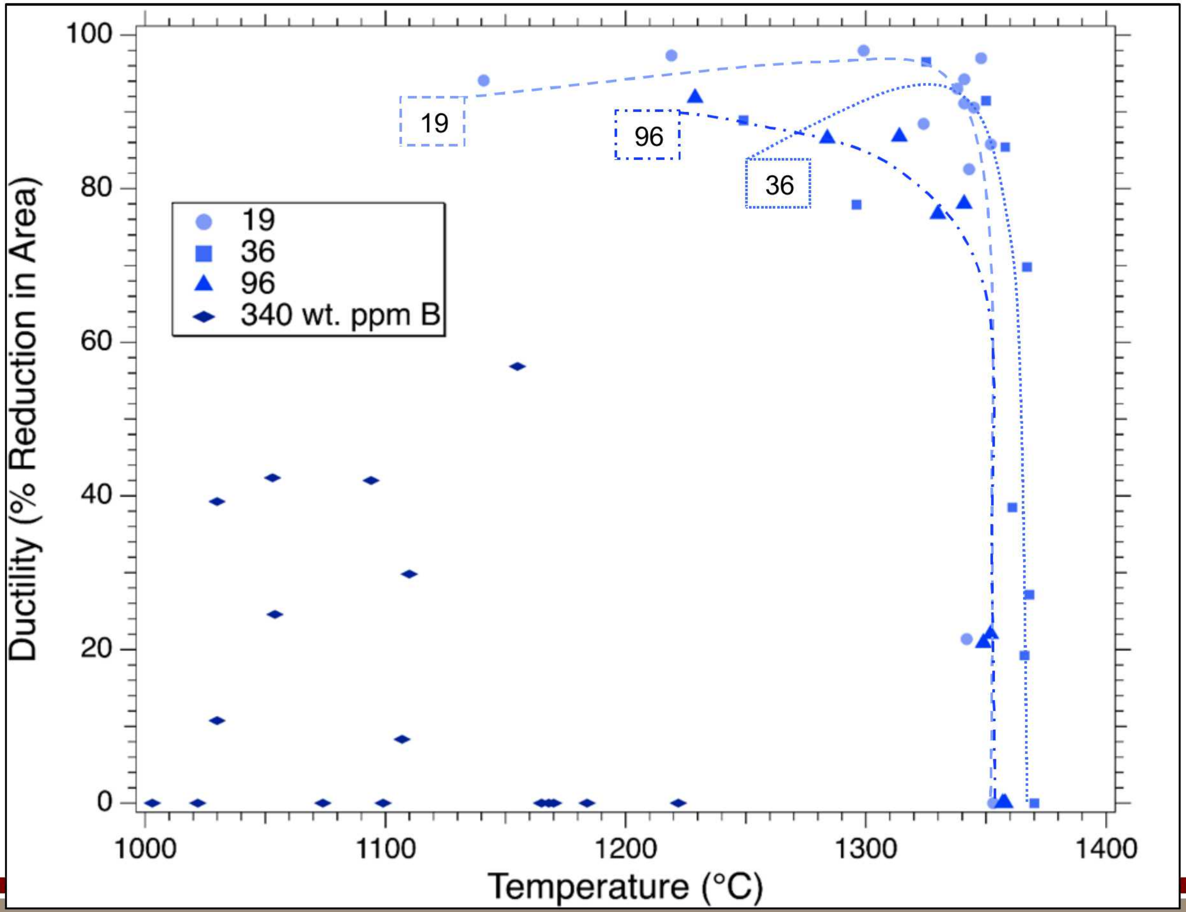

Hot ductility testing does not indicate liquation cracking risk for 304L with < 100 wt.ppm boron

- Boron-containing 304L with < 100 wt.ppm B shows similar ductility signature as commercial ASTM A276 304L with no B micro-alloying addition

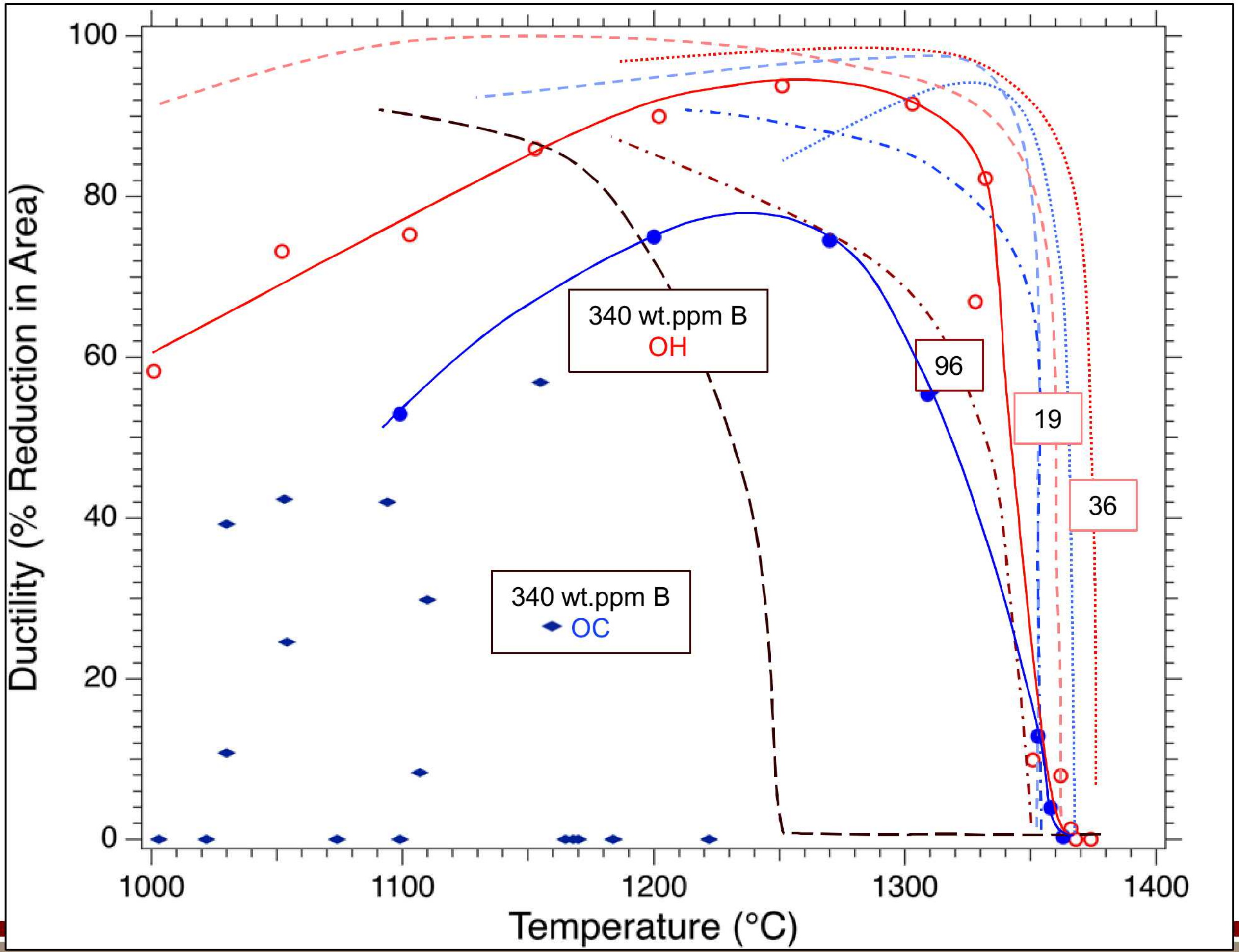

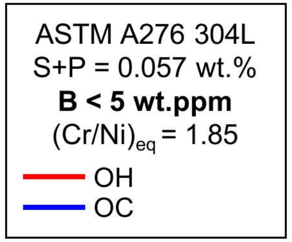

GTA Welds: Light optical microscopy

- Near fusion boundary HAZ liquation cracks only observed in highest B content condition
- Examination of autogenous GTA weld samples exhibits similar trend predicted by Gleeble hot ductility

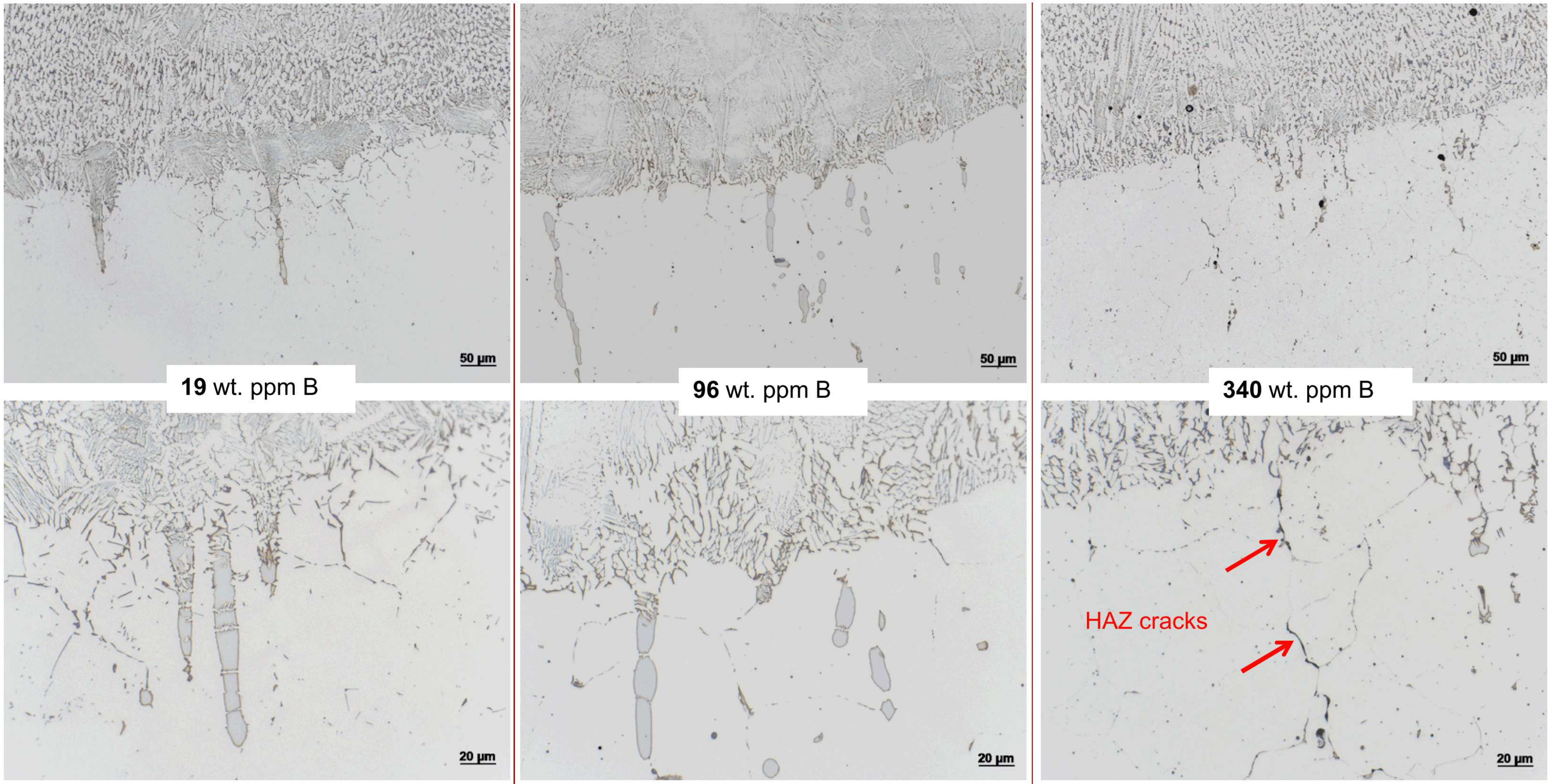

Etchant: 10% KOH electrolytic

GTA Welds: Electron Microscopy (340 wt. ppm B)

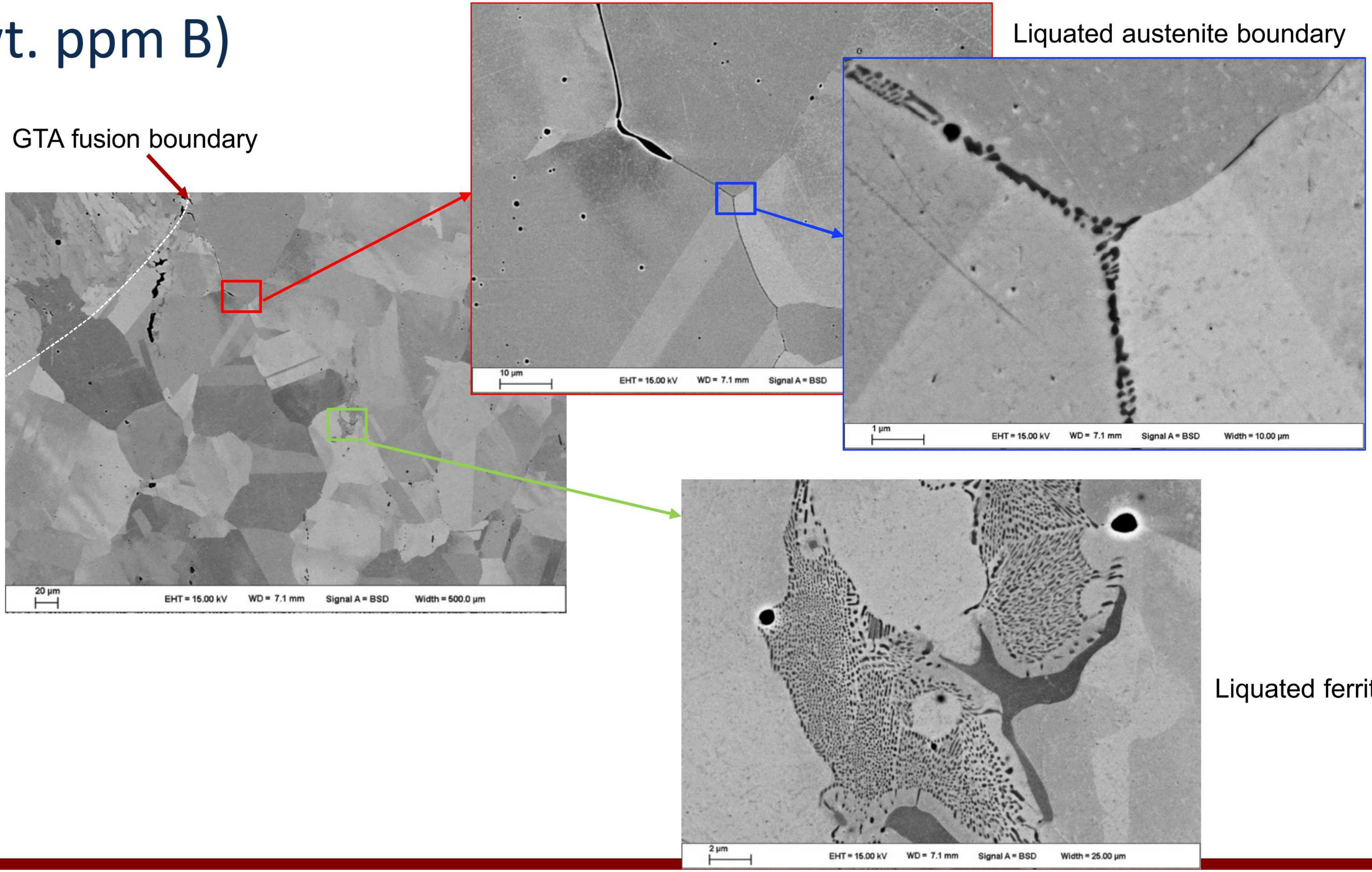

CW Laser Welds: Light Optical Microscopy

- Intermittent HAZ cracking observed in laser welds at significantly lower B content compared to autogenous GTA welds.

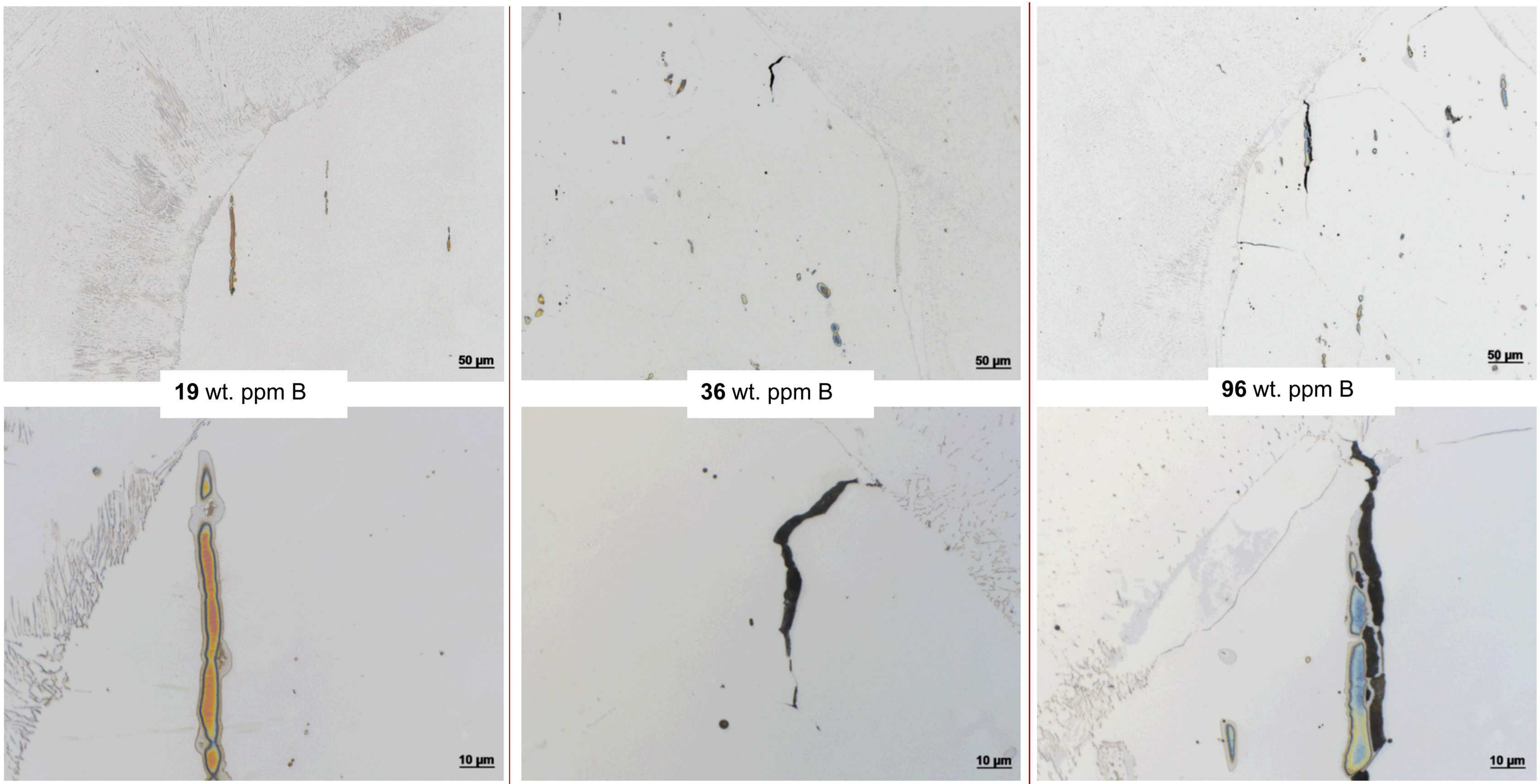

Etchant: 10% KOH electrolytic

CW Laser Weld: 340 wt.ppm B

- Extensive HAZ liquation cracking in highest B condition
- Weld metal solidification cracks also observed

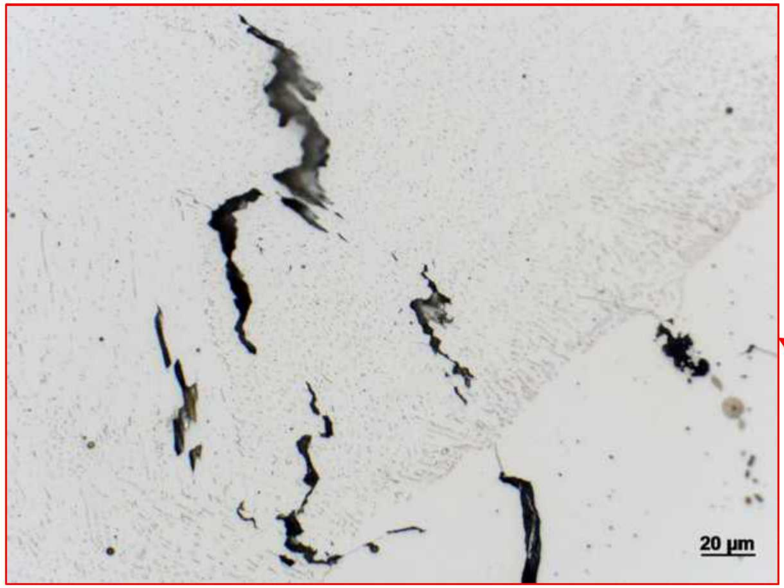

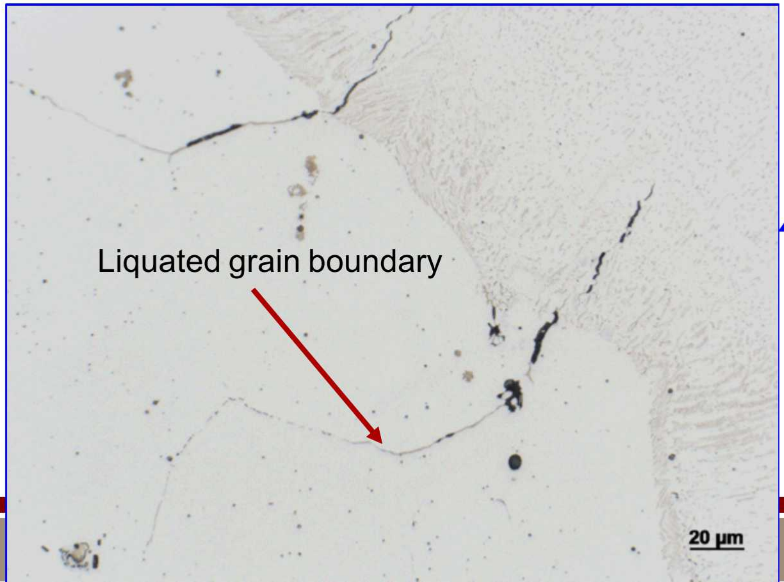

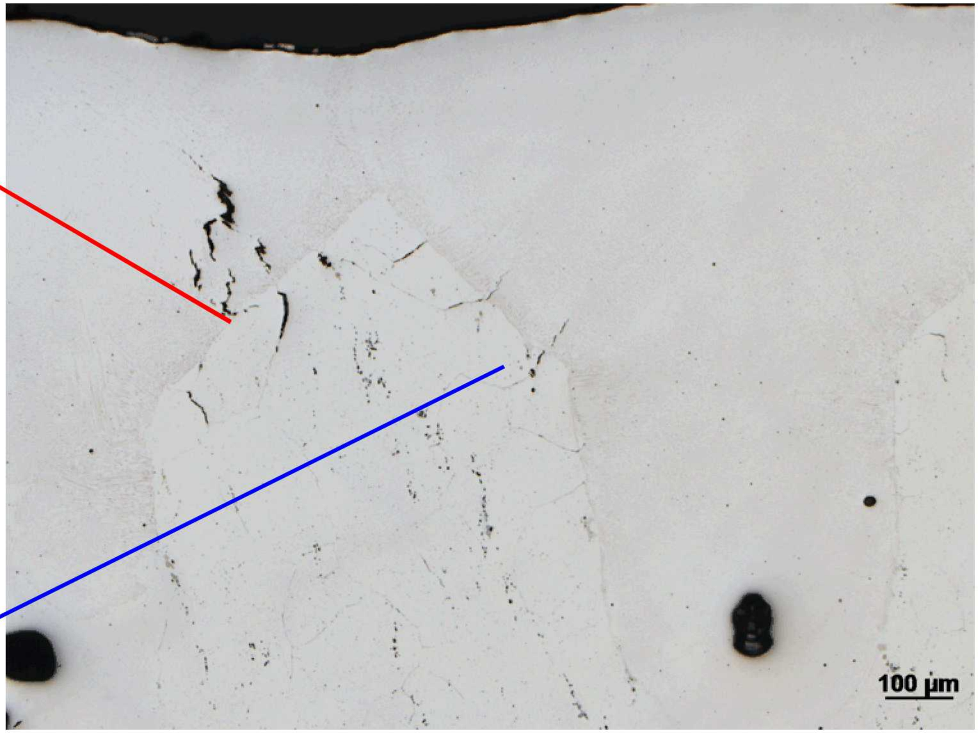

Etchant: 10% KOH electrolytic

CW Laser Weld: 340 wt.ppm B: Electron Microscopy

- High-resolution backscatter electron imaging reveals fine-scale microconstituent decorating liquated HAZ austenite grain boundaries
  - Eutectic structure considerably finer in LBW vs. GTA welds exhibiting liquation